Tests of lepton universality with semitauonic b-quark decays

Olivier Leroy

Tests of lepton universality with semitauonic b-quark decays

Olivier Leroy, on behalf of the LHCb collaboration

Aix Marseille Univ, CNRS/IN2P3, CPPM, Marseille, France

5 July 2018

XXXIX International Conference on High Energy Physics, COEX, Seoul, Korea

Outline

Introduction

- SM features Lepton Flavor Universality (**LFU**): equal electroweak coupling to all charged leptons. Branching ratios to e, μ and τ differ only due to their mass
- However, some deviations measured already at LEP

  $\frac{2\sigma(W\to\tau\nu_\tau)}{\sigma(W\to e\nu_e)+\sigma(W\to\mu\nu_\mu)} = 1.077 \pm 0.026$, 2.8σ above SM [arXiv:0511027]
- In this talk, tests LFU in semitauonic decays measuring the following ratios:

$$R(X_c) = \frac{\mathcal{B}(B\to X_c\tau^+\nu_\tau)}{\mathcal{B}(B\to X_c\mu^+\nu_\mu)}\,,\ X_c = D^* \text{ or } J/\psi$$

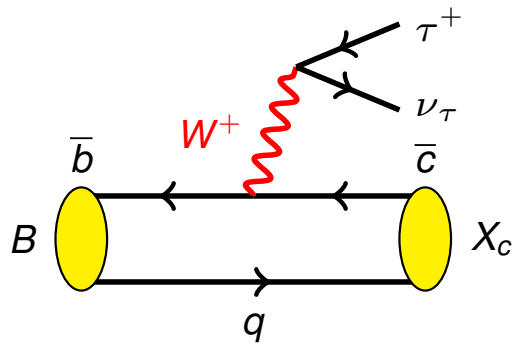

SM predictions:

- $R(D^*) = 0.258 \pm 0.005$ [HFLAV Summer 2018]
- $R(J/\psi) \in [0.25, 0.28]$

[PLB452 (1999) 120, arXiv:0211021, PRD73 (2006) 054024, PRD74 (2006) 074008]

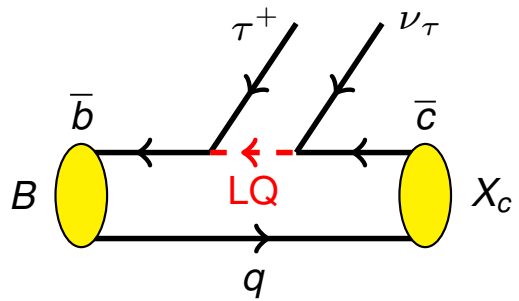

Ratios sensitive to possible NP coupling mainly to the 3rd generation

- Only LHCb Run 1 data, $3\,\text{fb}^{-1}$, 2011(12), $\sqrt{s} = 7(8)\,\text{TeV}$
- τ^+ is reconstructed either into $\mu^+\nu_\mu\bar{\nu}_\tau$ (muonic) or $3\pi(\pi^0)\bar{\nu}_\tau$ (hadronic) modes

$R(D^*)$ muonic [PRL 115, 112001 (2015)]

$R(D^*)$ muonic ($\tau^+ \to \mu^+ \nu_\mu \bar{\nu}_\tau$) [PRL 115, 112001 (2015)]

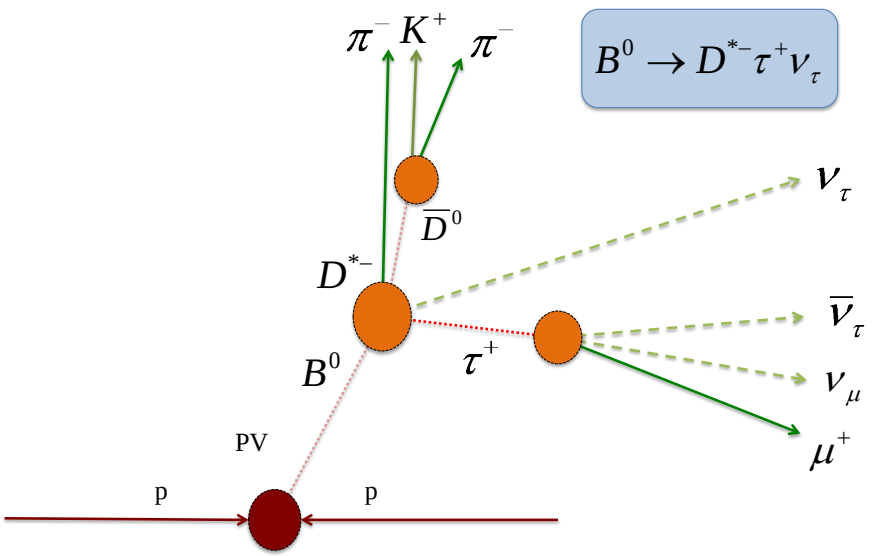

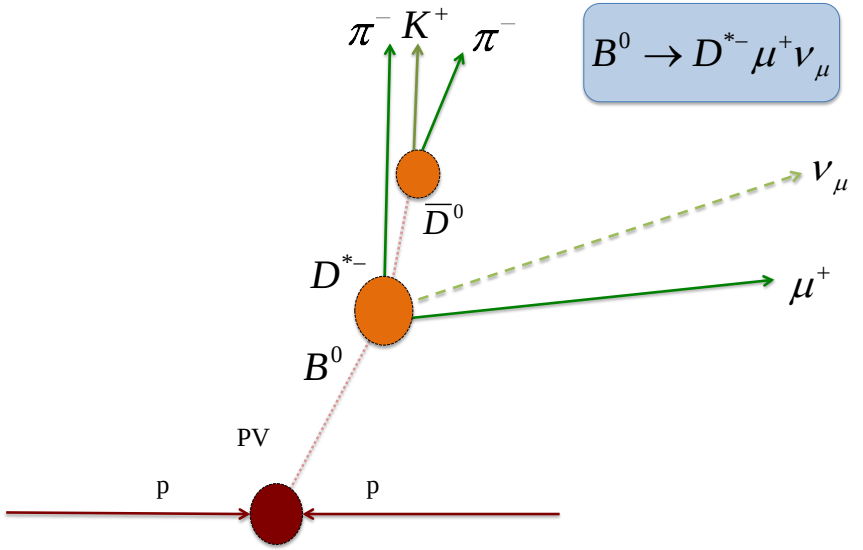

- $R(D^*) = \frac{\mathcal{B}(B^0 \to D^{*-} \tau^+ \nu_\tau)}{\mathcal{B}(B^0 \to D^{*-} \mu^+ \nu_\mu)}$ with $\tau^+ \to \mu^+ \nu_\mu \bar{\nu}_\tau$, $\mathcal{B}(\tau^+ \to \mu^+ \nu_\mu \bar{\nu}_\tau) = (17.39 \pm 0.04)\%$
- Normalization mode with the *same visible final state*
- 3 neutrinos for the signal mode and one for the normalisation: no narrow peak to fit
- Separate τ and μ via a 3D binned template fit, in the B rest frame, on:
  1. $m^2_{\text{miss}} = (p^\mu_B - p^\mu_{D^*} - p^\mu_\mu)^2$ missing mass squared
  2. E^*_μ muon energy
  3. $q^2 = (p^\mu_B - p^\mu_{D^*})^2$ squared 4-momentum transfer to the lepton system
- Background and signal shapes extracted from control samples and simulations validated against data

$R(D^*)$ muonic $(\tau^+ \to \mu^+ \nu_\mu \bar{\nu}_\tau)$ [PRL 115, 112001 (2015)]

- Signal more visible in the high q^2 bins (red)
- Backgrounds: feed-down from excited D states, double charm DD where one D decays semileptonically, combinatorial, muon mis-ID

$$R(D^*) = 0.336 \pm 0.027(\text{stat}) \pm 0.030(\text{syst})$$

1.9σ above SM

- Dominant systematics: size of simulation sample $\to$ will be improved in the next iteration

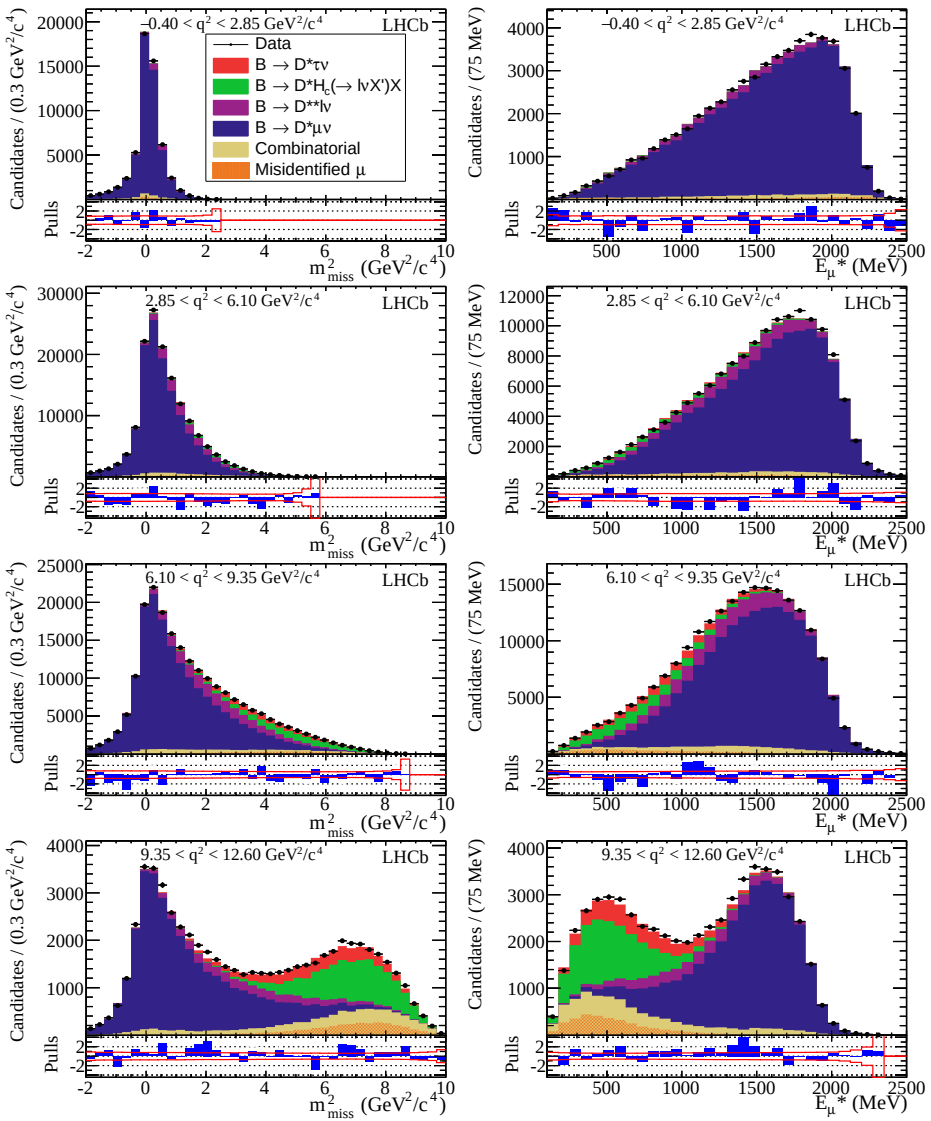

$R(D^*)$ hadronic [PRL 120, 171802 2018], [PRD 97,072013 2018]

$R(D^*)$ hadronic ($\tau \to 3\pi\nu_\tau$) [PRL 120, 171802 2018], [PRD 97,072013 2018]

We measure:

$$\mathcal{K}(D^*) = \frac{\mathcal{B}(B^0 \to D^{*-}\tau^+\nu_\tau)}{\mathcal{B}(B^0 \to D^{*-}3\pi)} = \frac{N_{D^*\tau\nu_\tau}}{N_{D^*3\pi}} \times \frac{\varepsilon_{D^*3\pi}}{\varepsilon_{D^*\tau\nu_\tau}} \times \frac{1}{\mathcal{B}(\tau^+ \to 3\pi(\pi^0)\bar{\nu}_\tau)}$$

- Signal and normalization modes chosen to have the same final state $D^{*-}3\pi$
- $\mathcal{B}(\tau \to 3\pi(\pi^0)\bar{\nu}_\tau) \simeq 13.9\%$
- τ^+ reconstructed into $\pi^+\pi^-\pi^+\bar{\nu}_\tau \Rightarrow$ we have the τ vertex!
- A semileptonic decay without (charged) lepton in final state!
  $\Rightarrow$ zero background from abundant semileptonic $B^0 \to D^{*-}\mu^+\nu_\mu X$ decays
- $N_{D^*3\pi}$ from an un-binned likelihood fit to $m(D^{*-}3\pi)$
- $N_{D^*\tau\nu_\tau}$ from a 3D template fit (t_τ, q^2, BDT)
- $R(D^*)$ obtained from:

$$R(D^*) \equiv \mathcal{K}(D^*) \times \frac{\mathcal{B}(B^0 \to D^{*-}3\pi)}{\mathcal{B}(B^0 \to D^{*-}\mu^+\nu_\mu)}$$

[$\sim$4% precision, BaBar, Belle, LHCb]

[$\sim$2% precision, HFLAV 2016]

$R(D^*)$ hadronic ($\tau \to 3\pi\nu_\tau$) [PRL 120, 171802 2018], [PRD 97,072013 2018]

Most abundant background $X_b \to D^{*-}3\pi X$ (BR $\sim 100\times$ signal) suppressed by requiring the τ vertex to be downstream wrt B vertex along beam direction

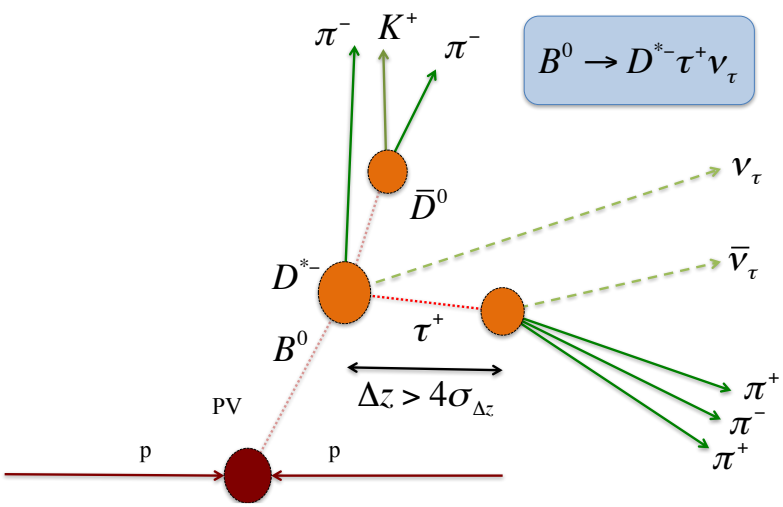

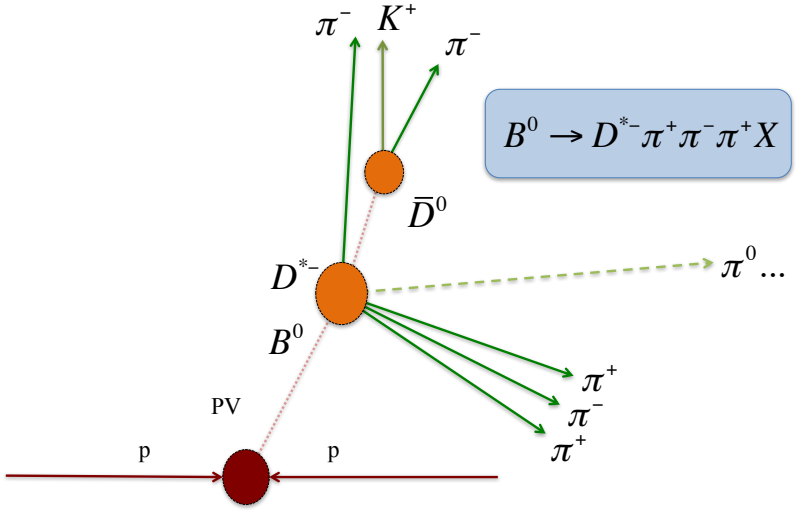

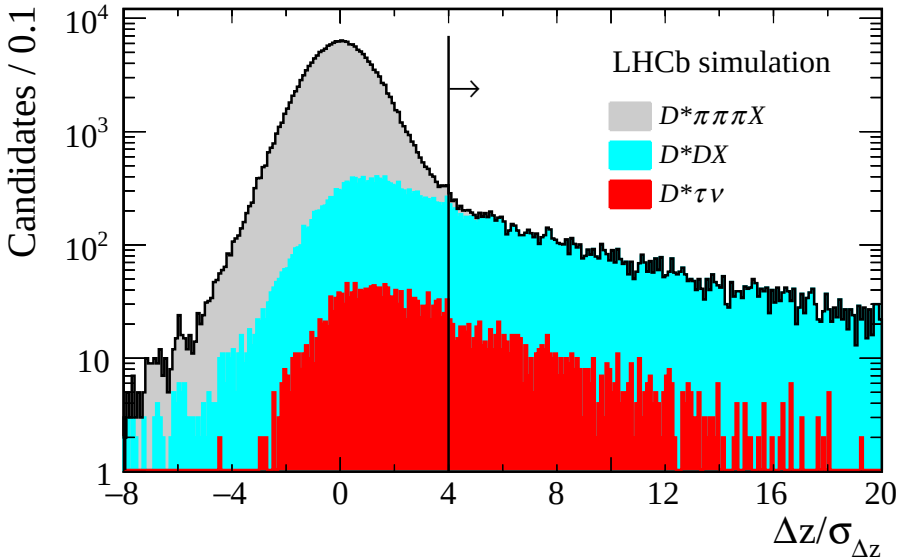

- $\Delta z > 4\sigma_{\Delta z}$ improves S/B by 160
- Remaining background due to doubly charmed decay with non-negligible lifetime:
  - $X_b \to D^* D_s^+ X \sim 10\times$ signal
  - $X_b \to D^* D^+ X \sim 1\times$ signal
  - $X_b \to D^* D^0 X \sim 0.2\times$ signal

$R(D^*)$ hadronic ($\tau \to 3\pi\nu_\tau$) [PRD 97,072013 2018]

Double charm background rejected with a **BDT** using the resonant structures of the $\tau^+ \to 3\pi\bar{\nu}_\nu$ and $D_s^+ \to 3\pi X$ decays

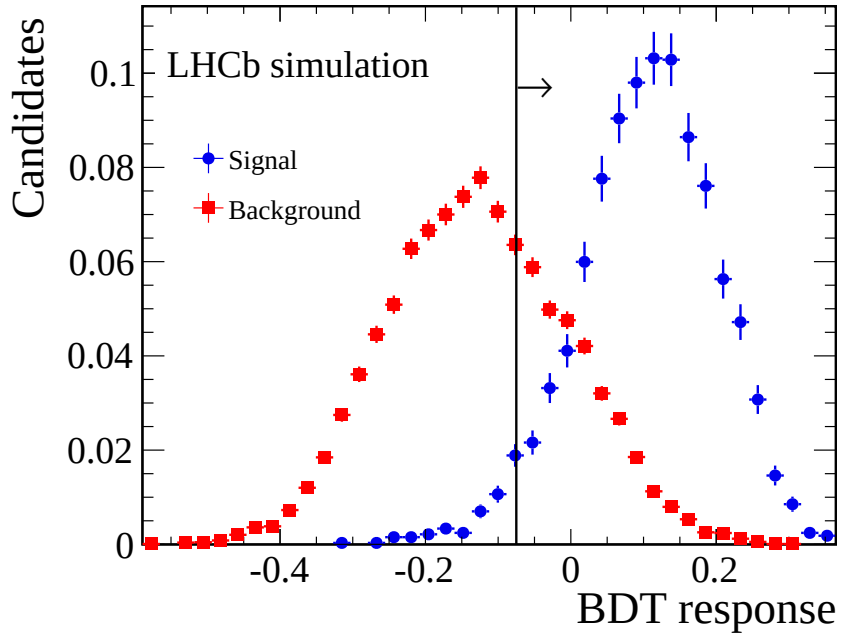

Different $X_b \to D^{*-} D_s^+ X$ contributions determined using $D_s^+ \to 3\pi$ decays.
Clear separation between D_s, D_s^* and D_s^{**}

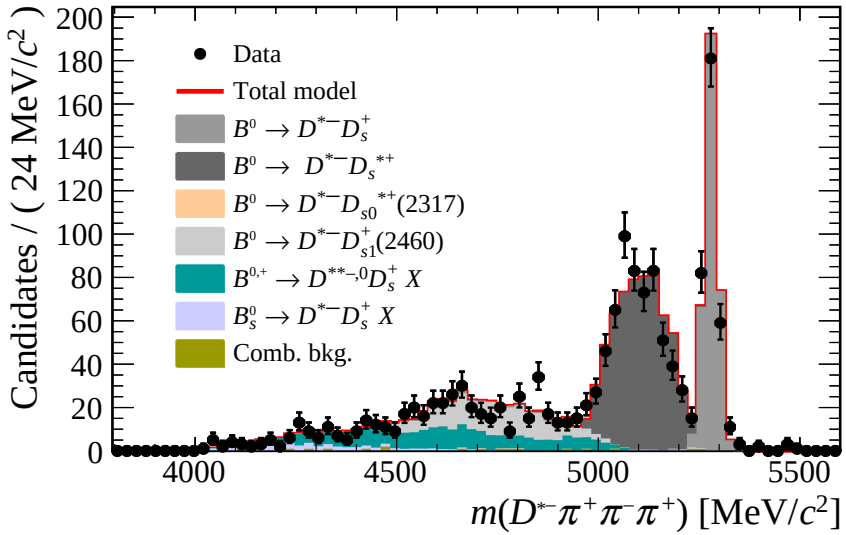

Fit to data for candidates containing a $D^{*-} D_s^+$ pair, where $D_s^+ \to 3\pi$.

$R(D^*)$ hadronic ($\tau \to 3\pi\nu_\tau$) [PRL 120, 171802 2018], [PRD 97,072013 2018]

- 3D template binned likelihood fit results presented for the 3π decay time and q^2 in 4 BDT bins
- Templates extracted from simulation and data control samples
- The increase in signal (red) purity as function of BDT output is clearly seen, as well as the decrease of the D_s^+ component (orange)
- The dominant background at high BDT output becomes the D^+ component (blue), with its distinctive long lifetime
- $N(B^0 \to D^{*-}\tau^+\nu_\tau) = 1296 \pm 86$

$$R(D^*) = 0.291 \pm 0.019(\text{stat}) \pm 0.026(\text{syst}) \pm 0.013(\text{ext})$$

0.9σ above SM

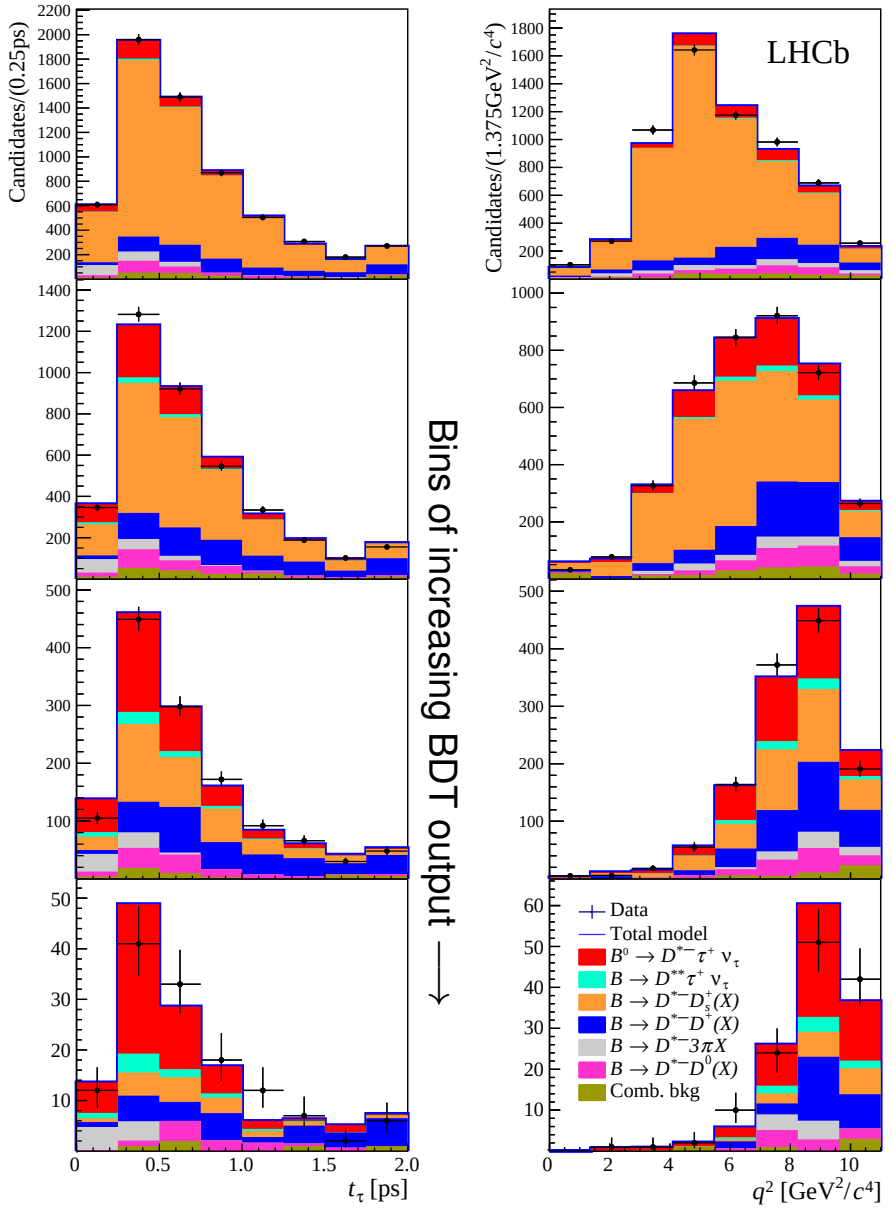

$R(D^*)$ hadronic ($\tau \to 3\pi\nu_\tau$) Systematics [PRL 120, 171802 2018]

$$R(D^*) = 0.291 \pm 0.019(\text{stat}) \pm 0.026(\text{syst}) \pm 0.013(\text{ext})$$

Breakdown of relative uncertainties:

Source	$\frac{\delta R(D^{*-})}{R(D^{*-})}$ [%]
Simulated sample size	4.7
Empty bins in templates	1.3
Signal decay model	1.8
$D^{**}\ \tau\ \nu$ and $D_s^{**}\ \tau\ \nu$ feed-downs	2.7
$D_s^+ \to 3\pi X$ decay model	2.5
$B \to D^{*-} D_s^+ X,\ D^{*-} D^+ X,\ D^{*-} D^0 X$ backgrounds	3.9
Combinatorial background	0.7
$B \to D^{*-} 3\pi X$ background	2.8
Efficiency ratio	3.9
Normalization channel efficiency (modeling of $B^0 \to D^{*-} 3\pi$)	2.0
Total systematic uncertainty	9.1
Statistical uncertainty	6.5
Total uncertainty	11.9

Will be improved in the next iteration of the analysis

$R(J/\psi)$ [PRL 120, 171802 2018]

$B_c^+ \to J/\psi \tau^+ \nu$: $R_{J/\psi}$ [PRL 120, 121801 (2018)]

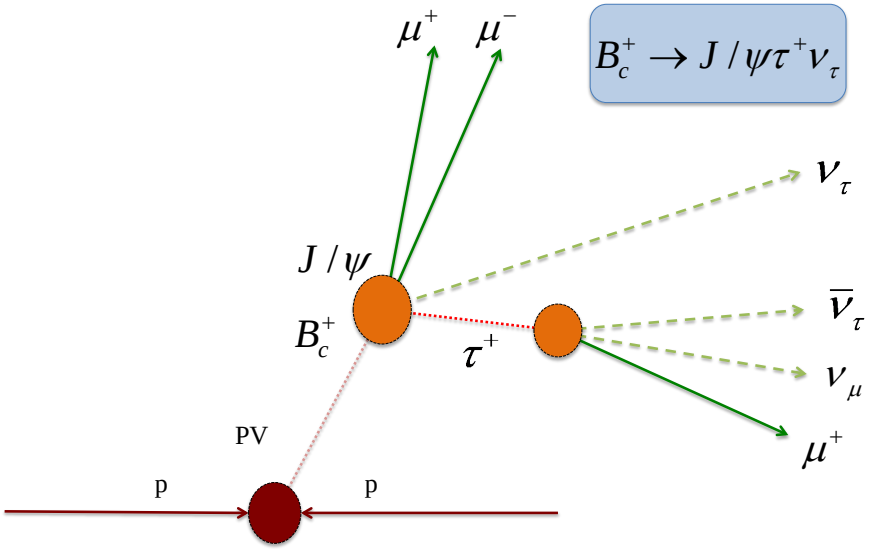

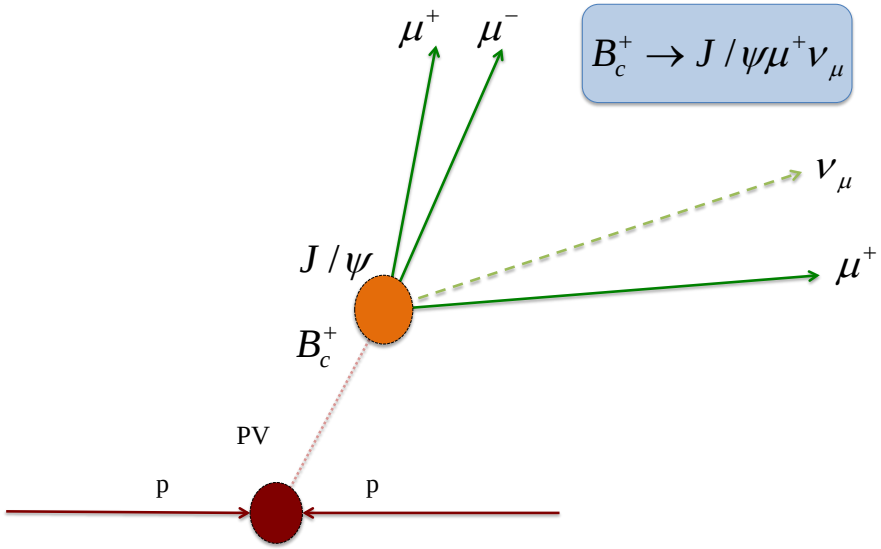

- $R(J/\psi) = \frac{\mathcal{B}(B_c^+ \to J/\psi\, \tau^+ \nu_\tau)}{\mathcal{B}(B_c^+ \to J/\psi\, \mu^+ \nu_\mu)}$, $\tau^+ \to \mu^+ \nu_\mu \bar{\nu}_\tau$
- B_c^+ decay form factors unconstrained experimentally: theoretical prediction not yet precise $R^{\text{theo}}(J/\psi) \in [0.25, 0.28]$

  [PLB452 (1999) 120, arXiv:0211021, PRD73 (2006) 054024, PRD74 (2006) 074008]
- Low B_c^+ production rate and short lifetime, but no "flying D background" and nice J/ψ
- Like in $R(D^*)$, use m^2_{miss}, E^*_μ and q^2. Add information from B_c^+ decay time

$B_c^+ \to J/\psi \tau^+ \nu$: $R_{J/\psi}$ [PRL 120, 121801 (2018)]

- 3D template binned fit
- Shapes of various components are represented by a template distribution derived from control samples or simulations validated against data
- Main background is $b \to J/\psi +$ mis-ID hadron
- First evidence for the decay $B_c^+ \to J/\psi \tau^+ \nu_\tau$ (3σ)

$$R(J/\psi) = 0.71 \pm 0.17(\text{stat}) \pm 0.18(\text{syst})$$

About 2σ above SM

- Main systematics: form factor and size of simulation sample

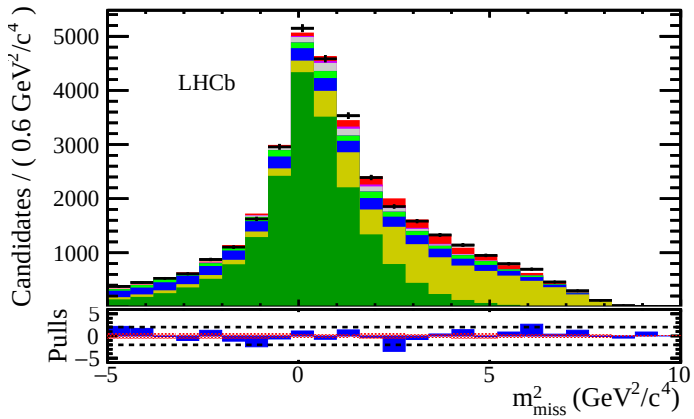

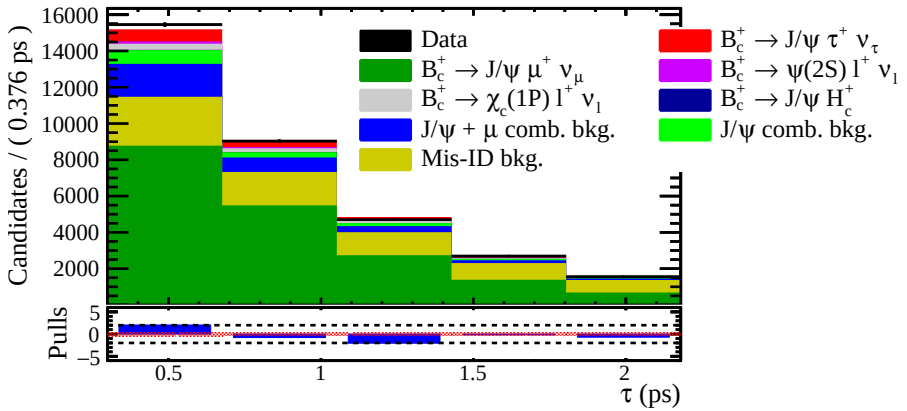

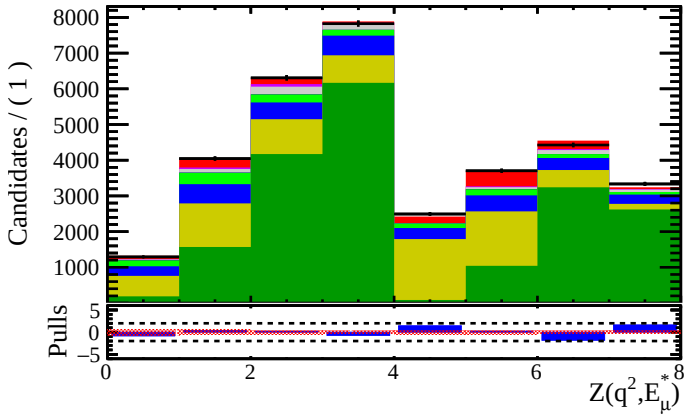

$R(D^*)$ and $R(J/\psi)$ summary

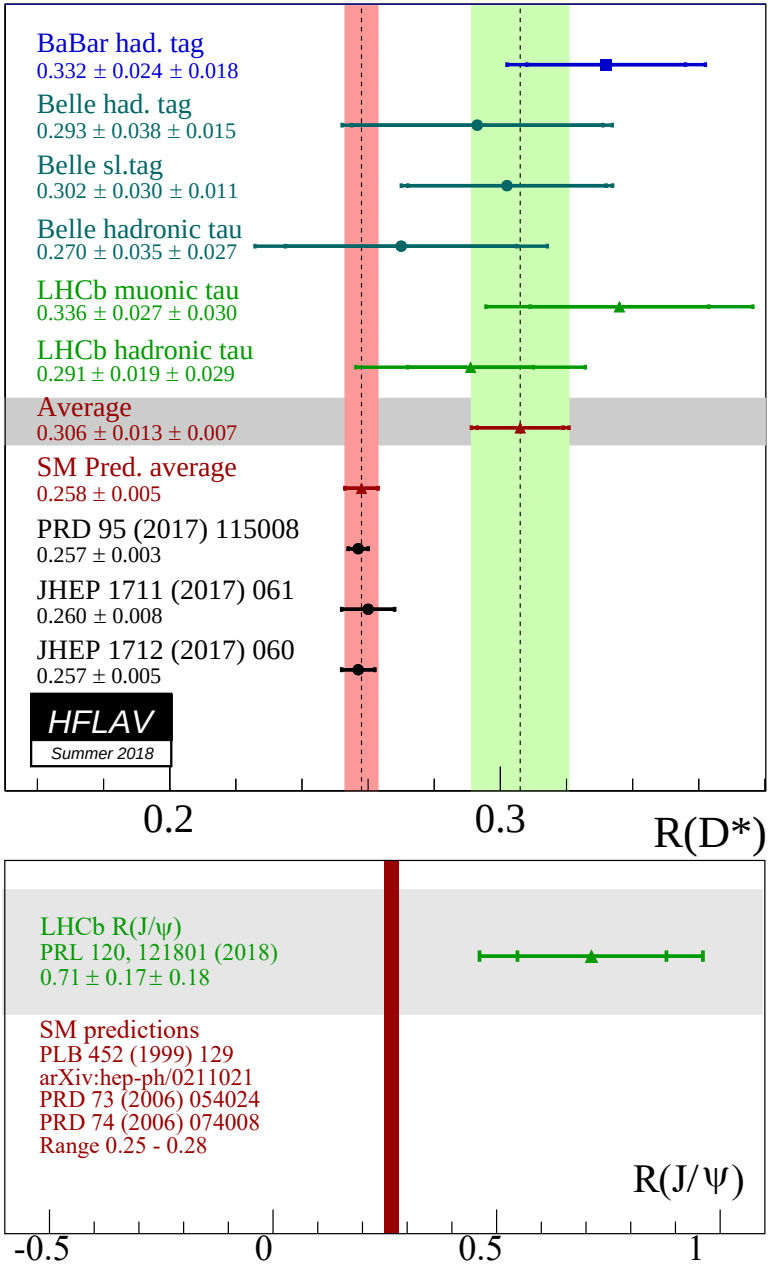

3 experiments, 7 measurements, different analysis techniques: ALL $R(D^*)$ and $R(J/\psi)$ measurements lie ABOVE the SM expectations.

$R(D^*)$ average 3.0σ above the SM prediction [HFLAV]

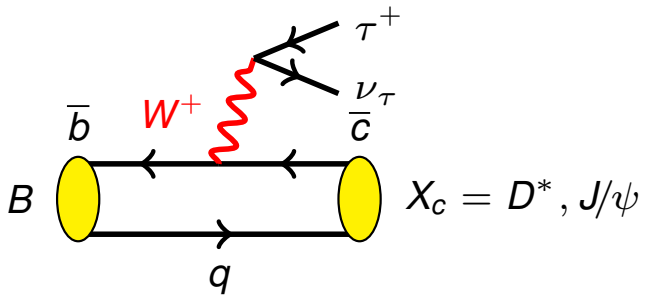

Possible NP contributions ?

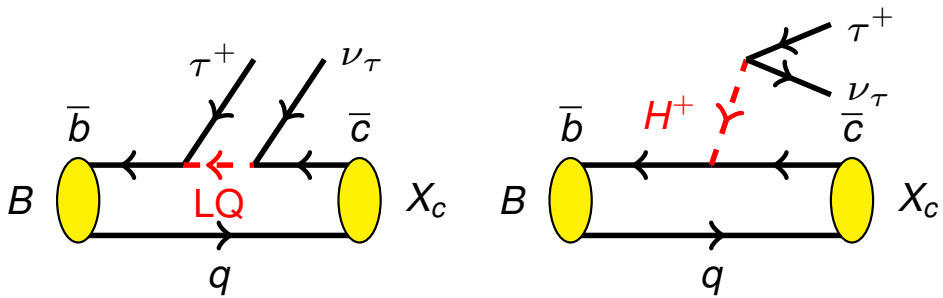

$R(D^*)$ and $R(J/\psi)$ summary (NEW at ICHEP 2018)

[Heavy Flavor Averaging Group, HFLAV]

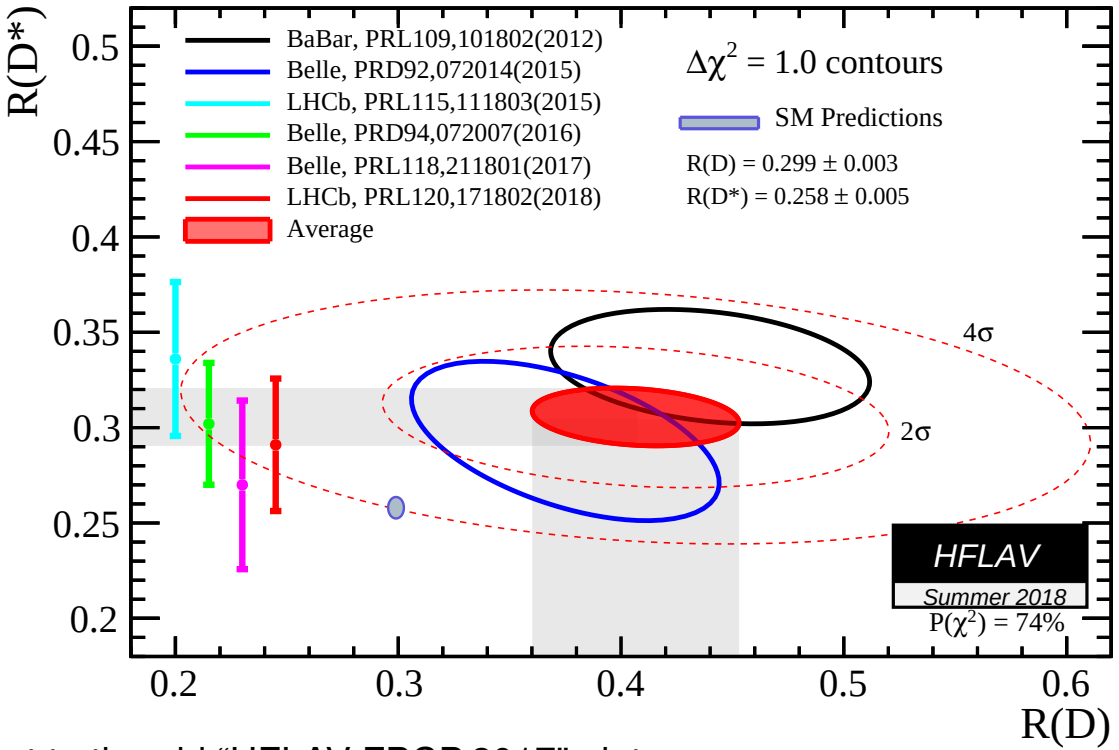

Three changes with respect to the old "HFLAV FPCP 2017" plot:

- $R(D^*)$ SM prediction changed from 0.252 ± 0.002 [PRD85, 094025 (2012)] to 0.0258 ± 0.005 [PRD95, 115008 (2017)], [JHEP 1711 (2017) 061], [JHEP 1712 (2017) 060]
- $R(D)$ SM prediction changed from 0.300 ± 0.008 to 0.299 ± 0.003 [PRD94, 094008 (2016)] [PRD95, 115008 (2017)], [JHEP 1712 (2017) 060], [PRD92, 034506 (2015)], [PRD92, 054410 (2015)]
- $R(D^*)$ experimental value changed from 0.304 to 0.306, following a tiny change between preliminary and published LHCb hadronic analysis.

$\Rightarrow$ Overall tension slightly reduced (was 4.1σ) but still **3.8σ away from the SM!**

Conclusions and prospects

- Three $b \to c\tau\nu$ tests of LFU with semitauonic analyses so far in LHCb: $R(D^*)$ muonic, $R(D^*)$ hadronic and $R(J/\psi)$ muonic.
- LHCb average $R(D^*) = 0.310 \pm 0.0155(\text{stat}) \pm 0.0219(\text{syst})$
  1.9σ above the SM prediction, dominated by the hadronic mode.
- **3.8σ tension in $R(D)$ - $R(D^*)$** when combining BaBar, Belle and LHCb.
  2σ discrepancy in $B_c^+ \to J/\psi\tau^+\nu$ goes in the same direction.
- Measurements presented performed with Run 1. Run 2 will bring a factor 5 in statistics, then Run 3, 4, 5 and plans until 2037!
- Many systematics will reduce with larger samples. Other will benefit from BESSIII and Belle II measurements.
- Many more analyses to come:
  - $b \to c\tau\nu$: $R(D^+)$, $R(D^0)$, $R(D_s^{(*)-})$, $R(\Lambda_c^{(*)})$, ...
  - $b \to u\tau\nu$: $R(\Lambda_b^0 \to p\tau\nu)$, $R(B \to pp\tau\nu)$, ...

  Interest will then shift towards new observables beyond the branching fraction ratios, e.g. angular analysis to determine spin structure of potential NP.
- Exciting work-plan in the coming years,
  with crucial interplay between experiments and theory.

Backups

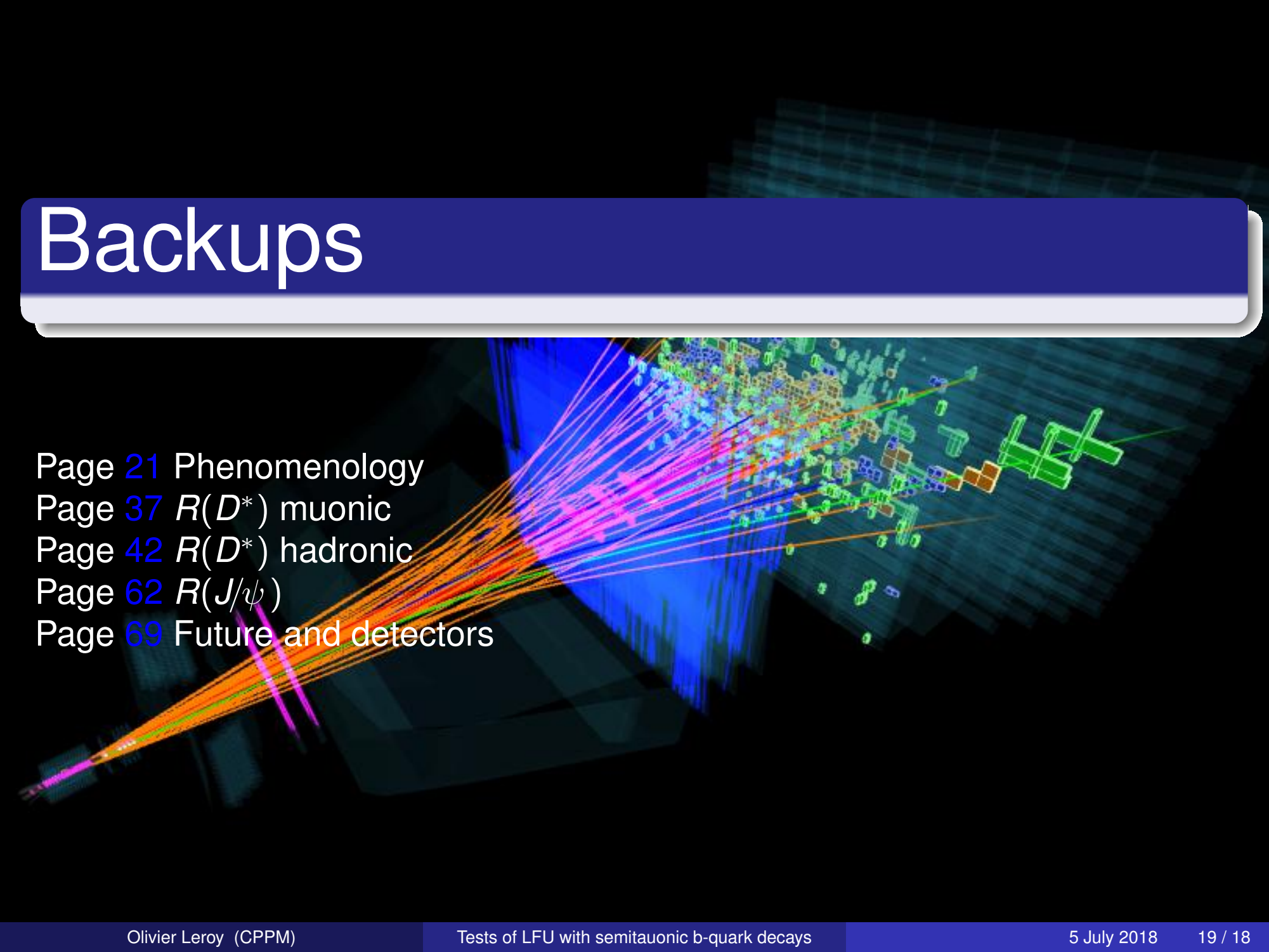

More on LFU

Let's go back ~ 100 years, and suppose we can test matter only with long wave-length photons...

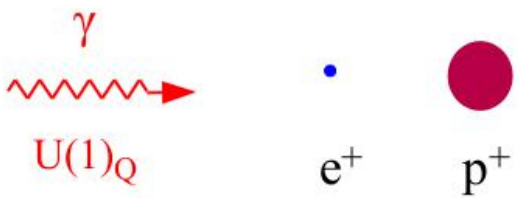

These two particles seems to be "identical copies" but for their mass ...

That's exactly the same (misleading) argument we use to infer LFU...

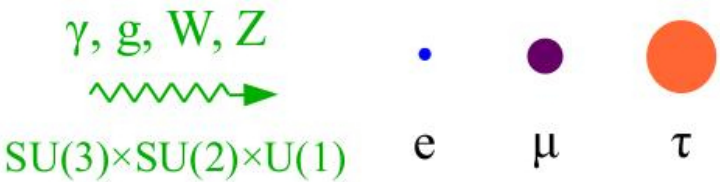

These three (families) of particles seems to be "identical copies" but for their mass ...

The SM quantum numbers of the three families could be an "accidental" low-energy property: the different families may well have a very different behavior at high energies, as signaled by their different mass

Tantalizing tensions with respect to the SM

Observable	Tension wrt SM	Limited by
$B \to D^{(*)}\tau\nu / B \to D^{(*)}\ell\nu,\ \ell = \mu, e$	3.8σ	experiment
$(g-2)_\mu$	3.6σ	exp. & theo.
$B^0 \to K^{*0}\mu\mu$ angular dist., BR	3.4σ	exp. & theo.
$B_s^0 \to \phi\mu\mu$ BR	3.0σ	experiment
$2\sigma(W \to \tau\nu_\tau)/(\sigma(W \to e\nu_e) + \sigma(W \to \mu\nu_\mu))$	2.8σ	experiment
$B^+ \to K^+\mu\mu / B^+ \to K^+ee$	2.6σ	experiment
$B^0 \to K^{*0}\mu\mu / B^0 \to K^{*0}ee$	2.6σ	experiment
$B_c^+ \to J/\psi\,\tau^+\nu / B_c^+ \to J/\psi\,\mu^+\nu$	2.0σ	exp. & theo.

Many other interesting results exhibit no tension today, but put strong constraints on NP models.
They remain fundamental for future searches, e.g.: γ, B^0-D^0-K^0-mixing, ϕ_s, $\sin 2\beta$, $B_s^0 \to \mu\mu$, $B \to X_s\gamma$, V_{cb}, $B \to \tau\nu$, CPV in charm, CLVF, $K \to \pi\nu\bar{\nu}$, ...

Flavor Anomalies

- $b \to s\ell\ell$

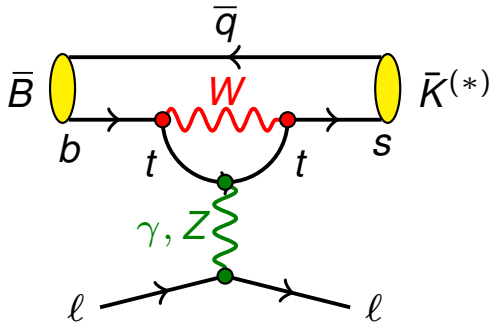

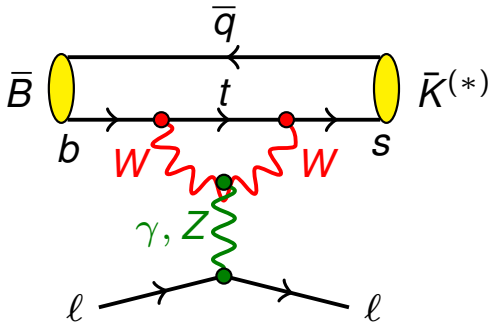

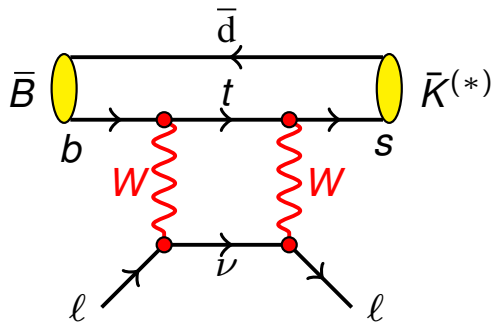

- $b \to c\tau\nu_\tau$

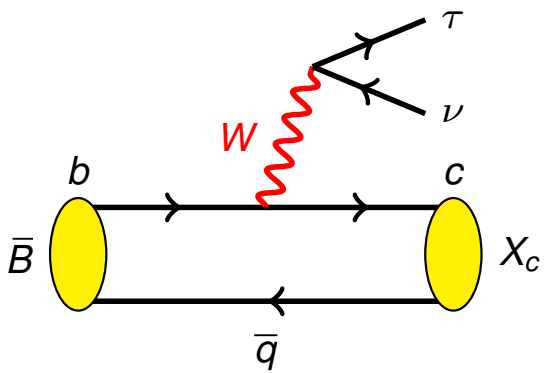

Effective field theory

Transition $B \to f$ described by an effective Hamiltonian $\langle f|\mathcal{H}_{\text{eff}}|B\rangle$, with

$$\mathcal{H}_{\text{eff}} = -\frac{4G_F}{\sqrt{2}} V_{tb} V_{tq}^* \sum_i \Big(\underbrace{C_i \mathcal{O}_i}_{\text{Left-handed}} + \underbrace{C_i' \mathcal{O}_i'}_{\text{Right-handed}} \Big)$$

Computed by splitting into:

- C_i (Wilson coefficients): short distance (perturbative) effective couplings, can be computed in terms of fundamental couplings of the SM and beyond
- $\langle f|\mathcal{O}_i|B\rangle$: long distance (non perturbative), computed using QCD at low energy or extracted by phenomenological analysis. $\mathcal{O}_i$ are local operators:

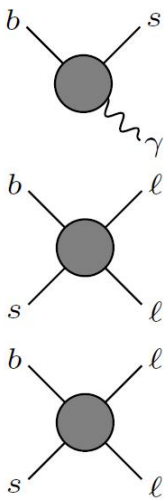

	$b \to s\gamma$	$B \to \mu\mu$	$b \to s\ell\ell$
$\mathcal{O}_7^{(\prime)}$ photon penguin	✓		✓
$\mathcal{O}_9^{(\prime)}$ vector coupling			✓
$\mathcal{O}_{10}^{(\prime)}$ axialvector coupling		✓	✓
$\mathcal{O}_{S,P}^{(\prime)}$ (pseudo)scalar penguin		✓	

Fundamental parameters of the Standard Model

The 28 parameters of the Standard Model are:

- the 3 coupling constant associated to $SU(2)_L \times U(1)_Y$ and $SU(3)_c$,
- the 2 Higgs field potential parameters μ and λ,
- the six quark masses and the six lepton masses,
- the four CKM parameters
- the six MNS parameters
- the possible QCD CP violating phase θ_{QCD}.

Two front LFU tests

- $R(K^{(*)}) = \mathcal{B}(B \to K^{(*)}\mu^+\mu^-)/\mathcal{B}(B \to K^{(*)}e^+e^-)$

  - **FCNC $b \to s\ell\ell$**
  - Rare decay forbidden at the tree level
  - Very sensitive to NP contributions in the loops

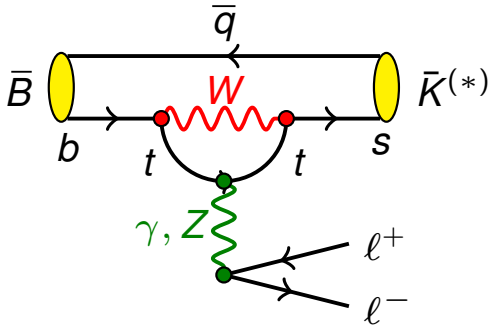

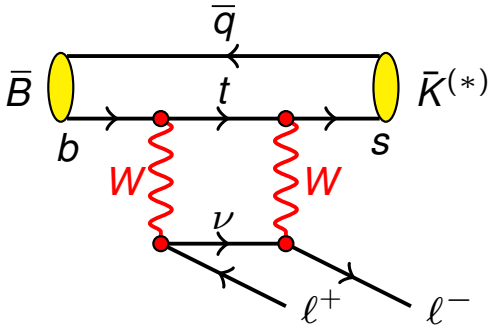

- $R(X_c) = \mathcal{B}(B \to X_c\tau^+\nu_\tau)/\mathcal{B}(B \to X_c\mu^+\nu_\mu)$, $X_c = D$, D^* or J/ψ

  - **Tree level $b \to c\tau\nu_\tau$**
  - Abundant semileptonic decay
  - Very well known in SM
  - Possible NP coupling mainly to the 3rd family

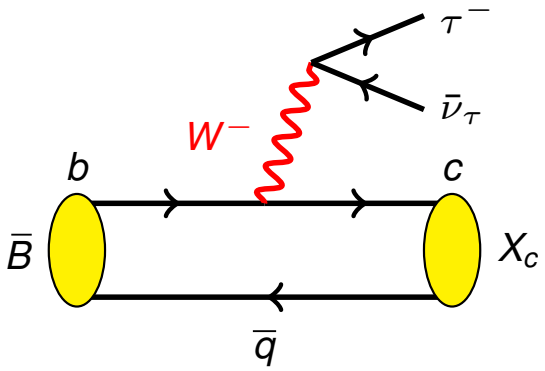

Two front LFU tests

- $R(K^{(*)}) = \mathcal{B}(B \to K^{(*)}\mu^+\mu^-)/\mathcal{B}(B \to K^{(*)}e^+e^-)$

  - **FCNC $b \to s\ell\ell$**
  - Rare decay forbidden at the tree level
  - Very sensitive to NP contributions in the loops

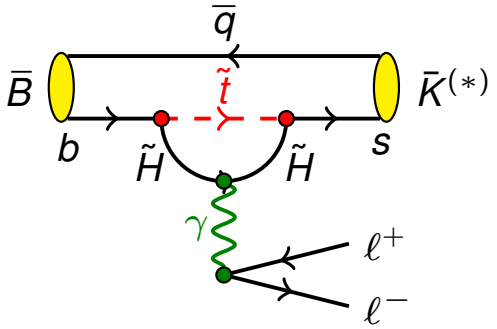

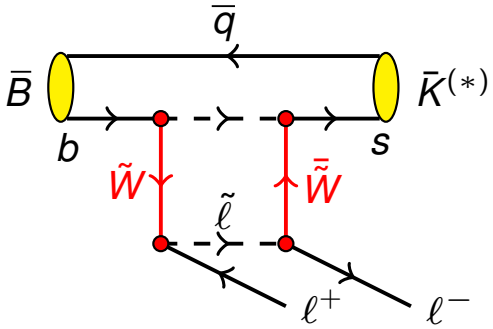

- $R(X_c) = \mathcal{B}(B \to X_c\tau^+\nu_\tau)/\mathcal{B}(B \to X_c\mu^+\nu_\mu)$, $X_c = D$, D^* or J/ψ

  - **Tree level $b \to c\tau\nu_\tau$**
  - Abundant semileptonic decay
  - Very well known in SM
  - Possible NP coupling mainly to the 3rd family

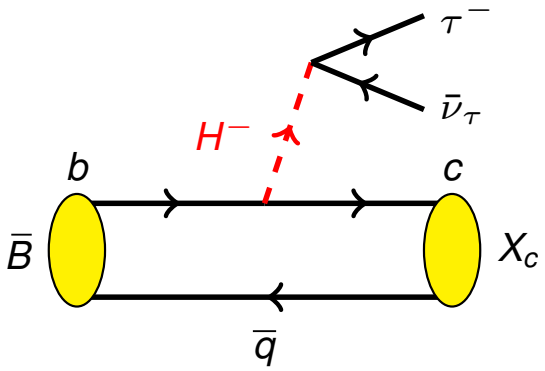

Lepton Flavor Universality in semileptonic decays

While semileptonic μ/e ratios are tested at 5% level by Belle:
$R(D)(\mu/e) = 0.995 \pm 0.022(\text{stat}) \pm 0.039(\text{syst})$ [Belle, PRD 93, 032006 (2016)]
$R(D^*)(\mu/e) = 0.96 \pm 0.05(\text{stat}) \pm 0.01(\text{syst})$ [Belle, 1702.01521]
we observe a $\sim$18% enhancement from the SM in the τ/μ ratio.

Full angular distribution in $B \to D^*(\to D\pi)\ell\bar{\nu}_\ell$

[D. Bečirević, S. Fajfer, I. Nišandžić, A. Tayduganov, arXiv:1602.03030]

The full angular distribution is given by

$$\frac{d^4\Gamma}{dq^2 d\cos\theta_\ell d\cos\theta_D d\chi} = \frac{3G_F^2|V_{cb}|^2}{256(2\pi)^4 m_B^3} q^2 \left(1-\frac{m_\ell^2}{q^2}\right)^2 \sqrt{\lambda_D^*(q^2)} \times B(D^* \to D\pi) \times \Big\{$$

$$[|H_+|^2 + |H_-|^2]\left(1+\cos^2\theta_\ell + \frac{m_\ell^2}{q^2}\sin^2\theta_\ell\right)\sin^2\theta_D + 2[|H_+|^2 - |H_-|^2]\cos\theta_\ell \sin^2\theta_D$$

$$+ 4|H_0|^2\left(\sin^2\theta_\ell + \frac{m_\ell^2}{q^2}\cos^2\theta_\ell\right)\cos^2\theta_D + 4|H_t|^2\frac{m_\ell^2}{q^2}\cos^2\theta_D$$

$$- 2\beta_\ell^2\left(\Re[H_+H_-^*]\cos 2\chi + \Im[H_+H_-^*]\sin 2\chi\right)\sin^2\theta_\ell\sin^2\theta_D$$

$$- \beta_\ell^2\left(\Re[H_+H_0^* + H_-H_0^*]\cos\chi + \Im[H_+H_0^* - H_-H_0^*]\sin\chi\right)\sin 2\theta_\ell \sin 2\theta_D$$

$$- 2\Re\left[H_+H_0^* - H_-H_0^* - \frac{m_\ell^2}{q^2}\left(H_+H_t^* + H_-H_t^*\right)\right]\cos\chi\sin\theta_\ell\sin 2\theta_D$$

$$- 2\Im\left[H_+H_0^* + H_-H_0^* - \frac{m_\ell^2}{q^2}\left(H_+H_t^* - H_-H_t^*\right)\right]\sin\chi\sin\theta_\ell\sin 2\theta_D$$

$$+ 8\Re[H_0H_t^*]\frac{m_\ell^2}{q^2}\cos\theta_\ell\cos^2\theta_D\Big\}, \quad \beta_\ell(q^2) = \sqrt{1-\frac{m_\ell^2}{q^2}}, \quad H(q^2) = \tilde{\varepsilon}^{\mu *}\langle D^*(\varepsilon)|J_\mu|\bar{B}\rangle$$

$B \to D^*(\to D\pi)\ell\bar{\nu}_\ell$: observables sensitive to NP

[D. Bečirević, S. Fajfer, I. Nišandžić, A. Tayduganov, arXiv:1602.03030]

What can be extracted from the proposed observables:

$d\Gamma/dq^2$	$\left[\lvert H_+\rvert^2 + \lvert H_-\rvert^2 + \lvert H_0\rvert^2\right]\left(1 + \frac{m_\ell^2}{2q^2}\right) + \frac{3}{2}\frac{m_\ell^2}{q^2}\lvert H_t\rvert^2$	
$1 - \mathcal{A}_{\lambda_\ell}$	$\lvert H_+\rvert^2 + \lvert H_-\rvert^2 + \lvert H_0\rvert^2 + 3\lvert H_t\rvert^2$	
$\mathcal{A}_{\rm FB}$	$\lvert H_+\rvert^2 - \lvert H_-\rvert^2 + 2\frac{m_\ell^2}{q^2}\Re\left[H_0 H_t^*\right]$	
$R_{L,T}$	$\lvert H_+\rvert^2 + \lvert H_-\rvert^2$	
A_5	$\lvert H_+\rvert^2 - \lvert H_-\rvert^2$	
C_χ	$\Re\left[H_+ H_-^*\right]$	
S_χ	$\Im\left[H_+ H_-^*\right]$	(=0 in the SM)
A_8	$\Im\left[(H_+ + H_-)H_0^* - \frac{m_\ell^2}{q^2}(H_+ - H_-)H_t^*\right]$	(=0 in the SM)
A_9	$\Re\left[(H_+ - H_-)H_0^* - \frac{m_\ell^2}{q^2}(H_+ + H_-)H_t^*\right]$	
A_{10}	$\Im\left[(H_+ - H_-)H_0^*\right]$	(=0 in the SM)
A_{11}	$\Re\left[(H_+ + H_-)H_0^*\right]$	

Best discriminating variable to NP

$$Heff = \frac{G_F}{\sqrt{2}} V_{cb} \left[(1 + g_V) \bar{c}\gamma_\mu b + (-1 + g_A) \bar{c}\gamma_\mu\gamma_5 b + g_S\, i\partial_\mu(\bar{c}b) + g_P\, i\partial_\mu(\bar{c}\gamma_5 b) + g_T\, i\partial_\nu(\bar{c} i\sigma_{\mu\nu} b) \right] (\bar{\ell}\gamma^\mu(1-\gamma_5)\nu_\ell)$$

[D. Bečirević, S. Fajfer, I. Nišandžić, A. Tayduganov, arXiv:1602.03030]

$\times$: "not sensitive"
$\star\star\star$: "maximally sensitive"

Quantity	g_V	g_A	g_S	g_P	g_T
$\mathcal{A}_{\rm FB}^{D}$	$\times$	–	$\star\star\star$	–	$\star$
$\mathcal{A}_{\lambda_\tau}^{D}$	$\times$	–	$\star\star\star$	–	$\star\star$
$\mathcal{A}_{\rm FB}^{D^*}$	$\star$	$\star\star\star$	–	$\star\star\star$	$\star$
$\mathcal{A}_{\lambda_\tau}^{D^*}$	$\times$	$\times$	–	$\star\star$	$\star$
$R_{L,T}$	$\times$	$\times$	–	$\star\star$	$\star\star$
A_5	$\star\star$	$\star\star$	–	$\star$	$\star\star\star$
C_χ	$\star$	$\times$	–	$\star\star$	$\star\star$
S_χ	$\star\star\star$	$\star\star\star$	–	$\times$	$\star\star\star$
A_8	$\star\star$	$\star\star$	–	$\star\star$	$\star\star\star$
A_9	$\star$	$\star$	–	$\star\star$	$\star\star$
A_{10}	$\star\star$	$\star\star$	–	$\times$	$\star\star$
A_{11}	$\times$	$\times$	–	$\star\star$	$\star\star$

SM expectation for $R(D^*)$ [S.Fajfer et al., PRD 85(2012) 094025]

$$\frac{d\Gamma_\ell}{dq^2} = \frac{G_F^2\,|V_{cb}|^2\,|\mathbf{p}|q^2}{96\pi^3 m_B^2}\left(1-\frac{m_\ell^2}{q^2}\right)^2 \times \left[\left(|H_{++}|^2+|H_{--}|^2+|H_{00}|^2\right)\left(1+\frac{m_\ell^2}{2q^2}\right)+\frac{3m_\ell^2}{2q^2}|H_{0t}|^2\right],$$

$q^2 = (p_B - p_{D^*})^2$ and $\mathbf{p}$ is the 3-mom of the D^* meson in the B rest frame:

$$|\mathbf{p}| = \frac{\sqrt{\lambda(m_B^2, m_{D^*}^2, q^2)}}{2m_B},\ \lambda(a,b,c) = a^2+b^2+c^2-2(ab+bc+ca).$$

H_{mn} are the hadronic helicity amplitudes:

$$\begin{aligned}
H_{\pm\pm}(q^2) =& (m_B + m_{D^*})A_1(q^2) \mp \frac{2m_B}{m_B+m_D^*}|\mathbf{p}|V(q^2),\\
H_{00}(q^2) =& \frac{1}{2m_{D^*}\sqrt{q^2}} \times \left[(m_B^2 - m_{D^*}^2 - q^2)(m_B+m_{D^*})A_1(q^2) - \frac{4m_B^2|\mathbf{p}|^2}{m_B+m_{D^*}}A_2(q^2)\right],\\
H_{0t}(q^2) =& \frac{2m_B|\mathbf{p}|}{\sqrt{q^2}}A_0(q^2),
\end{aligned}$$

$A_{0,1,2}(q^2)$, $V(q^2)$ are the the form factors.

SM expectation for $R(D^*)$ [S.Fajfer et al., PRD 85(2012) 094025]

To calculate these form factors it is useful to define the kinematical variable:

$$w = v_B \cdot v_{D^*} = \frac{m_B^2 + m_{D^*}^2 - q^2}{2 m_B m_{D^*}},$$

v_B, v_{D^*} are the four-velocities of B and D^*. It is possible to define $A_{0,1,2}(q^2)$, $V(q^2)$ in terms of four variables $h_{A_1}(w)$, $R_{0,1,2}(w)$:

$$A_1(q^2) = h_{A_1}(w)\frac{1}{2}(w+1)R, \tag{2a}$$

$$A_0(q^2) = \frac{R_0(w)}{R} h_{A_1}(w), \tag{2b}$$

$$A_2(q^2) = \frac{R_2(w)}{R} h_{A_1}(w), \tag{2c}$$

$$V(q^2) = \frac{R_1(w)}{R} h_{A_1}(w), \tag{2d}$$

where $R = 2\sqrt{m_B m_{D^*}}/(m_B + m_{D^*})$. According to the HQET computation of [CLN 1998], the w dependence of these quantities is given by:

$$h_{A_1}(w) = h_{A_1}(1)[1 - 8\rho^2 z + (53\rho^2 - 15)z^2 - (231\rho^2 - 91)z^3], \tag{3a}$$

$$R_0(w) = R_0(1) - 0.11(w-1) + 0.01(w-1)^2, \tag{3b}$$

$$R_2(w) = R_2(1) + 0.11(w-1) - 0.06(w-1)^2, \tag{3c}$$

$$R_1(w) = R_1(1) - 0.12(w-1) + 0.05(w-1)^2, \tag{3d}$$

with $z = (\sqrt{w+1} - \sqrt{2})/(\sqrt{w+1} + \sqrt{2})$.

SM expectation for $R(D^*)$ [S.Fajfer et al., PRD 85(2012) 094025]

$$R_{D^*}(q^2) = \frac{d\Gamma_\tau/dq^2}{d\Gamma_\ell/dq^2} =$$
$$= \left(1 - \frac{m_\tau^2}{q^2}\right)^2 \left[\left(1 + \frac{m_\tau^2}{2q^2}\right) + \frac{3m_\tau^2}{2q^2} \frac{|H_{0t}|^2}{|H_{++}|^2 + |H_{--}|^2 + |H_{00}|^2}\right]$$

where $d\Gamma_\ell/dq^2$ has been calculated in an analogous way to $d\Gamma_\tau/dq^2$.
Integrating over q^2 gives $R(D^*)$.

Citing HFLAV: New calculations are available since the 2017. The most relevant input to these new calculations are: form factors obtained fitting with the [BGL 1995] parameterization the unfolded spectrum from Belle [arXiv:1702.01521]. These new calculations are in good agreement between each other, and consistent with the old predictions for $R(D^*)$, but more robust. There are differences in the evaluation of the theoretical uncertainty associated mainly to assumptions on the pseudoscalar Form Factor. The central values of the SM predictions, and their uncertainty estimates, will evolve as more precise measurements of $B \to D^* \ell\nu$ spectra are available and new calculations are available. The disagreement on the treatment of the theoretical uncertaitines can be settled down when calculation of the $B \to D^*$ Form Factors beyond the zero recoil limit as well as information on the pseudoscalar Form Factor will be available.

	$R(D)$	$R(D^*)$
D.Bigi, P.Gambino, Phys.Rev. D94 (2016) no.9, 094008 [arXiv:1606.08030 [hep-ex]]	0.299 ± 0.003	
F.Bernlochner, Z.Ligeti, M.Papucci, D.Robinson, Phys.Rev. D95 (2017) no.11, 115008 [arXiv:1703.05330 [hep-ex]	0.299 ± 0.003	0.257 ± 0.003
D.Bigi, P.Gambino, S.Schacht, JHEP 1711 (2017) 061 [arXiv:1707.09509 [hep-ex]]		0.260 ± 0.008
S.Jaiswal, S.Nandi, S.K.Patra, JHEP 1712 (2017) 060 [arXiv:1707.09977 [hep-ex]]	0.299 ± 0.004	0.257 ± 0.005
Arithmetic average	$\mathbf{0.299 \pm 0.003}$	$\mathbf{0.258 \pm 0.005}$

The arithmetic average is used only for illustration and doesn't imply consent from the authors of the calculations. The SM uncertainty is currently subject to debate that HFLAV is following without taking a stance in this.

$R(D^*)$ and $R(D)$ summary

- Similarly to $R(D^*)$, the ratio is defined for D^- mesons:

$$R(D) = \frac{\mathcal{B}(B^0 \to D^- \tau^+ \nu_\tau)}{\mathcal{B}(B^0 \to D^- \ell^+ \nu_\ell)}$$

  and has been measured by Belle and BaBar
- Theoretical predictions: $R(D) = 0.299 \pm 0.003$

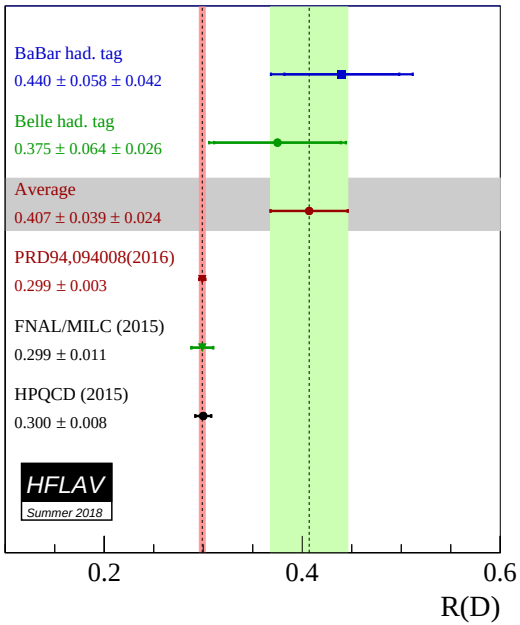

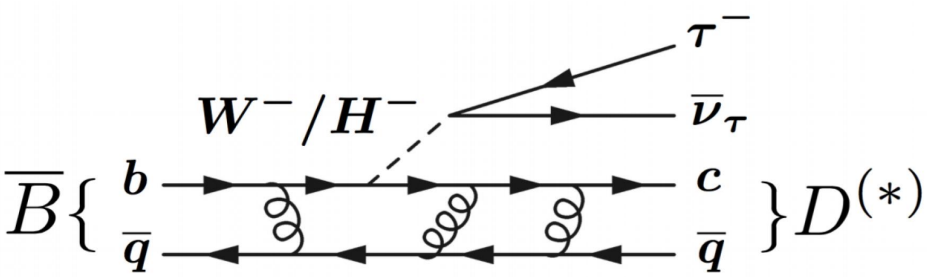

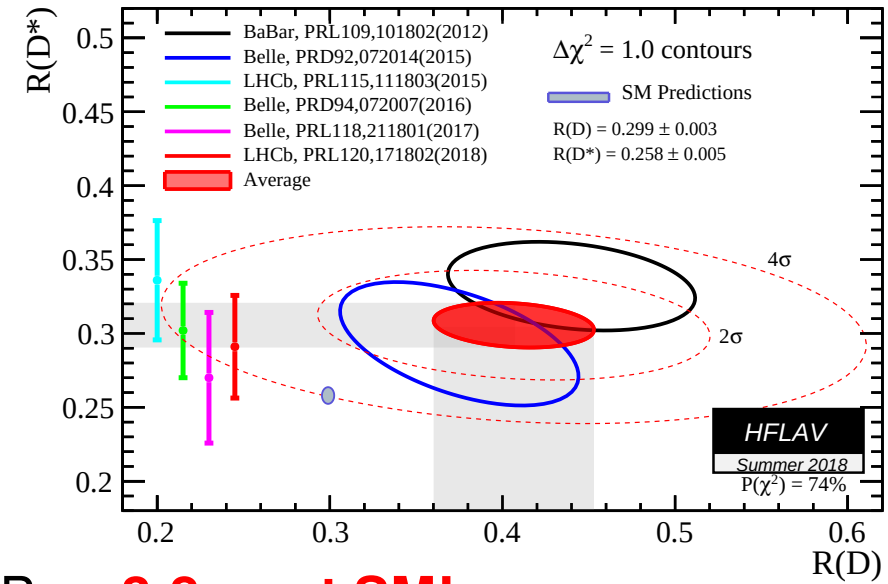

- Combination of LHCb, Belle and BaBar: **3.8σ wrt SM!**

Properties of charged leptons

Particle	Mass (MeV/c^2)	Lifetime	Main decay modes
e^-	0.5109989461(31)	>6.6$\times 10^{26}$ years	None
μ^-	105.6583745(24)	2.1969811(22) μs	$e^- \bar{\nu}_e \nu_\mu$
τ^-	1776.86(12)	290.3(5) fs	$\pi^- \pi^0 \nu_\tau$ (25.5%) $e^- \bar{\nu}_e \nu_\tau$ (17.8%) $\mu^- \bar{\nu}_\mu \nu_\tau$ (17.39%) $\pi^- \nu_\tau$ (10.8%) $\pi^- \pi^+ \pi^- \nu_\tau$ (9.3%)

D^* branching ratios

Mode	BR
$D^*(2007)^0 \to D^0\pi^0$	$(64.7 \pm 0.9)\%$
$D^*(2007)^0 \to D^0\gamma$	$(35.3 \pm 0.9)\%$
$D^*(2010)^+ \to D^0\pi^+$	$(67.7 \pm 0.5)\%$
$D^*(2010)^+ \to D^+\pi^0$	$(30.7 \pm 0.5)\%$
$D^*(2010)^+ \to D^+\gamma$	$(1.6 \pm 0.4)\%$

Particle	Mass (MeV/c^2)	Lifetime
D^+	1869.65 ± 0.05	(1.040 ± 0.007) ps
D^0	1864.83 ± 0.05	(0.4101 ± 0.0015) ps
D_s^+	1968.34 ± 0.07	(0.504 ± 0.004) ps
Λ_c^+	2286.46 ± 0.14	(0.200 ± 0.006) ps
$D^*(2007)^0$	2006.85 ± 0.05	-
$D^*(2010)^-$	2010.26 ± 26	-

τ lepton Branching Ratios [PDG 2018]

Mode	BR (%)
$\tau^- \to \pi^- \pi^0 \nu_\tau$	25.49 ± 0.09
$\tau^- \to e^- \bar{\nu}_e \nu_\tau$	17.82 ± 0.04
$\tau^- \to \mu^- \bar{\nu}_\mu \nu_\tau$	17.39 ± 0.04
$\tau^- \to \pi^- \nu_\tau$	10.82 ± 0.05
$\tau^- \to \pi^- \pi^+ \pi^- \nu_\tau$	9.31 ± 0.05
$\tau^- \to \pi^- \pi^+ \pi^- \pi^0 \nu_\tau$	4.62 ± 0.05

$R(D^*)$ muonic ($\tau^+ \to \mu^+ \nu_\mu \bar{\nu}_\tau$

$R(D^*)$ muonic $(\tau^+ \to \mu^+ \nu_\mu \bar{\nu}_\tau)$ [PRL 115 (2015) 112001]

$$R(D^*) = \frac{\mathcal{B}(B^0 \to D^{*-} \tau^+ \nu_\tau)}{\mathcal{B}(B^0 \to D^{*-} \mu^+ \nu_\mu)}$$
with $\tau^+ \to \mu^+ \nu_\mu \bar{\nu}_\tau$

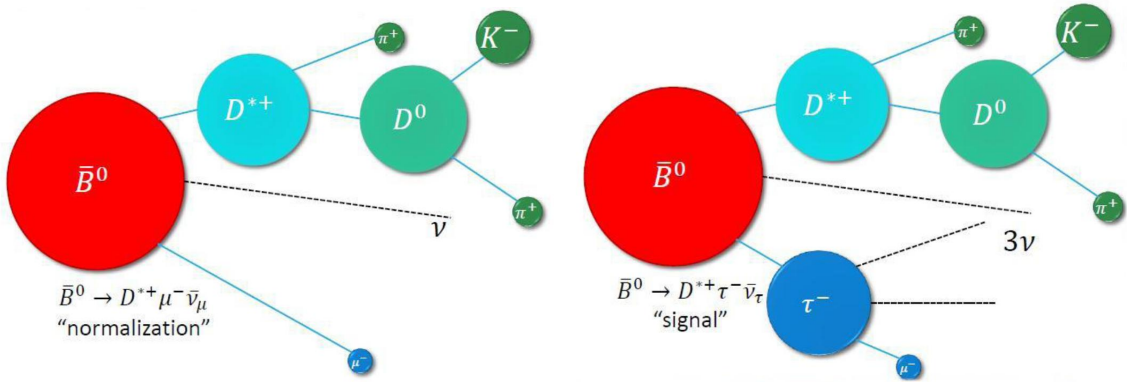

- Precise SM prediction: $R(D^*) = 0.258 \pm 0.005$ [HFLAV]
- Normalization mode with the *same visible final state*
- $\mathcal{B}(\tau^+ \to \mu^+ \nu_\mu \bar{\nu}_\tau) = (17.39 \pm 0.04)\%$
- Neutrinos: no narrow peak to fit
- Separate τ and μ via a $3D$ binned template fit, in the B rest frame, on:
  1. $m^2_{\text{miss}} = (p^\mu_B - p^\mu_{D^*} - p^\mu_\mu)^2$
  2. E^*_μ
  3. $q^2 = (p^\mu_B - p^\mu_{D^*})^2$
- Background and signal shapes extracted from control samples and simulations validated against data

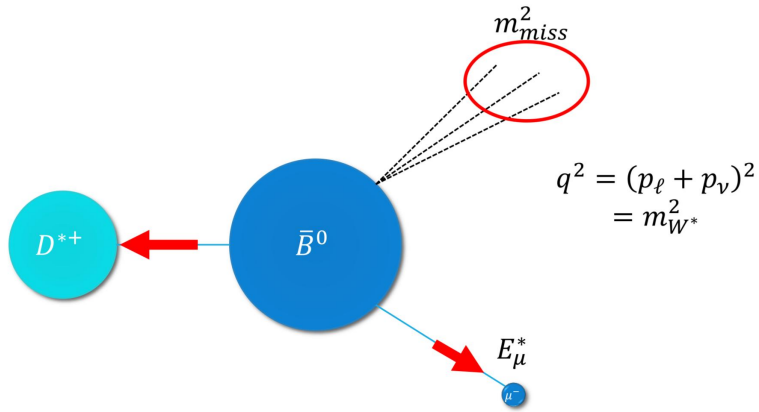

$R(D^*)$ muonic ($\tau^+ \to \mu^+ \nu_\mu \bar{\nu}_\tau$) [PRL 115 (2015) 112001]

Problem of missing neutrino: no analytical solution for p_B.
Approximate B momemtum $p_B^z = \frac{m_B}{m_{D\mu}} p_{D\mu}^z$.
m_B is the known B mass, $m_{D\mu}$ is the reconstructed one.
i.e. we approximate the B momentum by its visible one and we exploit the measured B flight trajectory.
This leads to $\sim$18% resolution on q^2, $m^2_{\rm miss}$ and E^*_μ, enough to preserve the discrimining feature of the original variables.

$R(D^*)$ muonic $(\tau^+ \to \mu^+ \nu_\mu \bar{\nu}_\tau)$ [PRL 115 (2015) 112001]

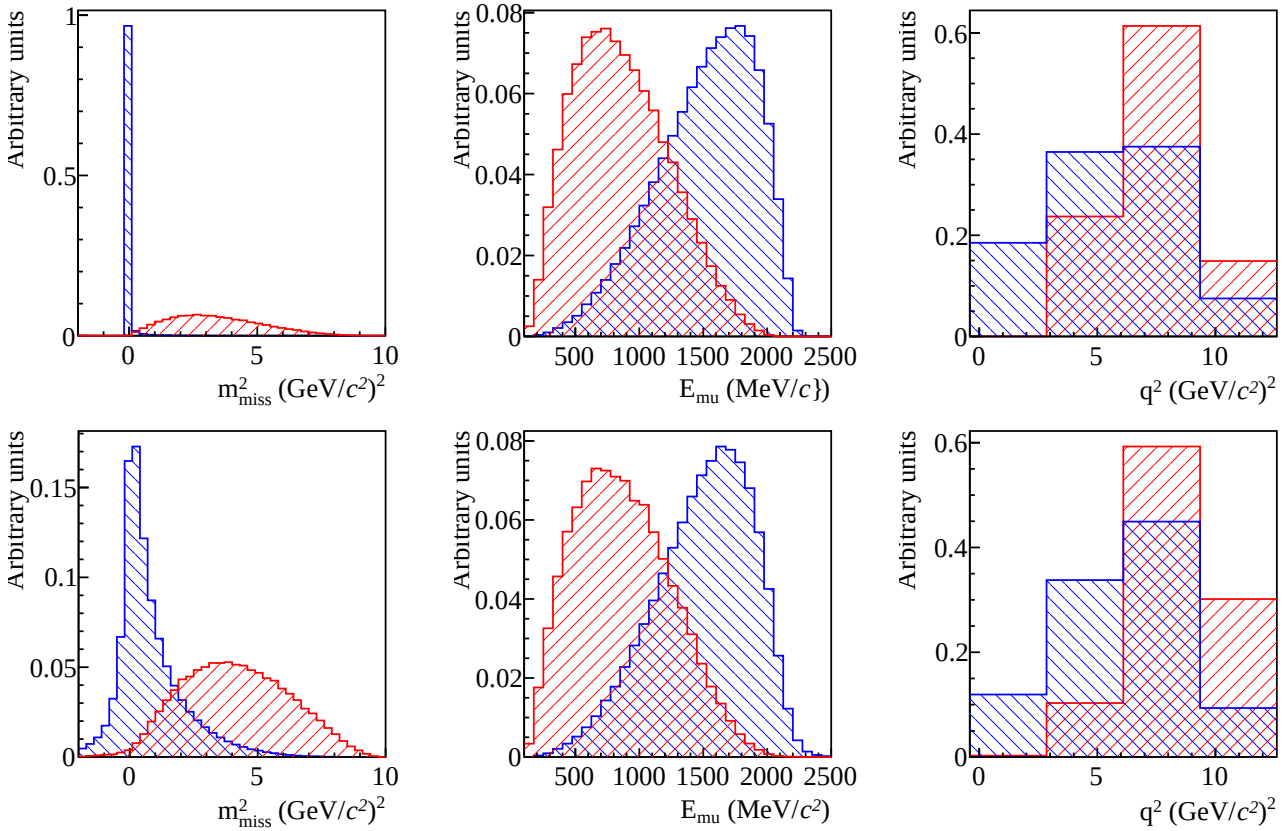

	$D^*\tau\nu_\tau$	$D^*\mu\nu_\mu$
m^2_{miss}	> 0	$\simeq 0$
E^*_μ	softer	harder
q^2	$> m^2_\tau$	> 0

Signal(red) and normalization mode (blue) using truth(top) and reconstructed(bottom) quantities

In the B rest frame:

- $m^2_{\text{miss}} = (p^\mu_B - p^\mu_{D*} - p^\mu_\mu)^2$: missing mass squared
- E^*_μ : muon energy
- $q^2 = (p^\mu_B - p^\mu_{D*})^2$: squared of the 4-mom transfered to the lepton system

$R(D^*)$ muonic ($\tau^+ \to \mu^+ \nu_\mu \bar{\nu}_\tau$) [PRL 115 (2015) 112001]

Model uncertainties	**Absolute size ($\times 10^{-2}$)**
Simulated sample size	2.0
Misidentified μ template shape	1.6
$\bar{B}^0 \to D^{*+}(\tau^-/\mu^-)\overline{\nu}$ form factors	0.6
$\bar{B} \to D^{*+} H_c(\to \mu\nu X')X$ shape corrections	0.5
$\mathcal{B}(\bar{B} \to D^{**}\tau^-\overline{\nu}_\tau)/\mathcal{B}(\bar{B} \to D^{**}\mu^-\overline{\nu}_\mu)$	0.5
$\bar{B} \to D^{**}(\to D^*\pi\pi)\mu\nu$ shape corrections	0.4
Corrections to simulation	0.4
Combinatorial background shape	0.3
$\bar{B} \to D^{**}(\to D^{*+}\pi)\mu^-\overline{\nu}_\mu$ form factors	0.3
$\bar{B} \to D^{*+}(D_s \to \tau\nu)X$ fraction	0.1
Total model uncertainty	**2.8**
Normalization uncertainties	**Absolute size ($\times 10^{-2}$)**
Simulated sample size	0.6
Hardware trigger efficiency	0.6
Particle identification efficiencies	0.3
Form-factors	0.2
$\mathcal{B}(\tau^- \to \mu^-\overline{\nu}_\mu\nu_\tau)$	< 0.1
Total normalization uncertainty	**0.9**
Total systematic uncertainty	**3.0**

$R(D^*)$ hadronic ($\tau \to 3\pi\nu_\tau$)

$R(D^*)$ hadronic ($\tau \to 3\pi\nu_\tau$) [PRD 97,072013 2018]

$$R(D^*) = \mathcal{K}(D^*) \times \frac{\mathcal{B}(B^0 \to D^{*-} 3\pi)}{\mathcal{B}(B^0 \to D^{*-} \mu^+ \nu_\mu)}$$

$$\text{with } \mathcal{K}(D^*) = \frac{\mathcal{B}(B^0 \to D^{*-} \tau^+ \nu_\tau)}{\mathcal{B}(B^0 \to D^{*-} 3\pi)} = \frac{N_{D^* \tau \nu_\tau}}{N_{D^* 3\pi}} \times \frac{\varepsilon_{D^* 3\pi}}{\varepsilon_{D^* \tau \nu_\tau}} \times \frac{1}{\mathcal{B}(\tau^+ \to 3\pi(\pi^0)\bar{\nu}_\tau)}$$

- Signal and normalization modes chosen to have the same final state
- $\mathcal{B}(\tau^+ \to \pi^+\pi^-\pi^+\bar{\nu}_\tau) = (9.31 \pm 0.05)\%$
- $\mathcal{B}(\tau^+ \to \pi^+\pi^-\pi^+\pi^0\bar{\nu}_\tau) = (4.62 \pm 0.05)\%$
- $N_{D^* 3\pi}$ from unbinned fit to $D^* 3\pi$ invariant mass
- $N_{D^* \tau \nu_\tau}$ from binned templated fit
- $\mathcal{B}(B^0 \to D^{*-} 3\pi)$ from [BaBar, PRD94 (2016) 091101] ($\sim$4% precision)
- $\mathcal{B}(B^0 \to D^{*-} \mu^+ \nu_\mu)$ from PDG ($\sim$2% precision)

$R(D^*)$ hadronic ($\tau \to 3\pi\nu_\tau$) [PRD 97,072013 2018]

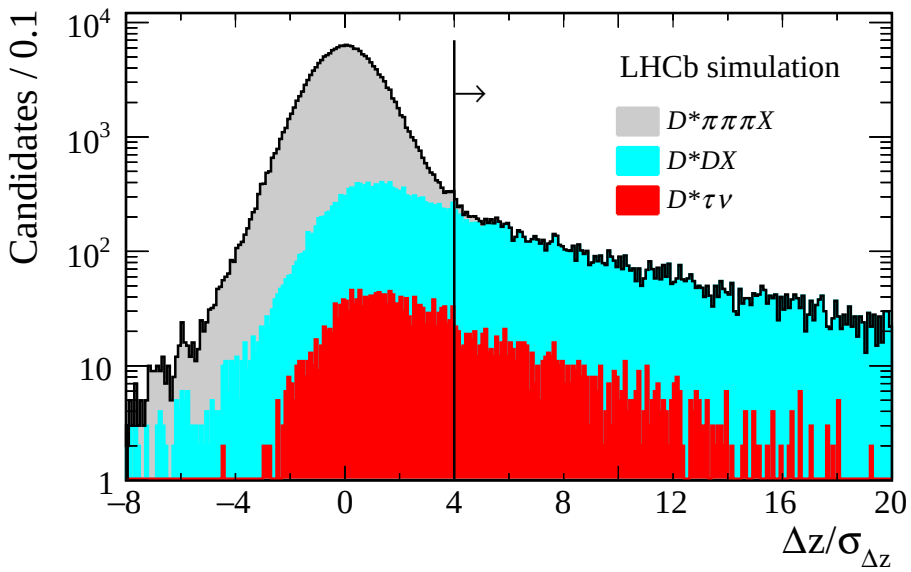

Distribution of the distance between the B^0 vertex and the 3π vertex along the beam direction, divided by its uncertainty, obtained using simulation. The grey area corresponds to the prompt background component, the cyan and red areas to double-charm and signal components, respectively. The vertical line shows the 4σ requirement used in the analysis to reject the prompt background component

$R(D^*)$ hadronic ($\tau \to 3\pi\nu_\tau$) [PRL 120, 171802 2018], [PRD 97,072013 2018]

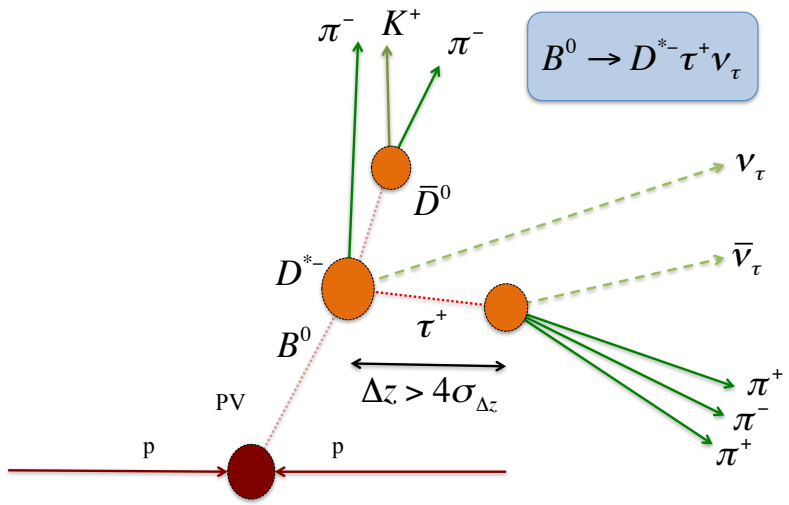

$R(D^*)$ hadronic ($\tau \to 3\pi\nu_\tau$). Anti-D_s^+ BDT [PRD 97,072013 2018]

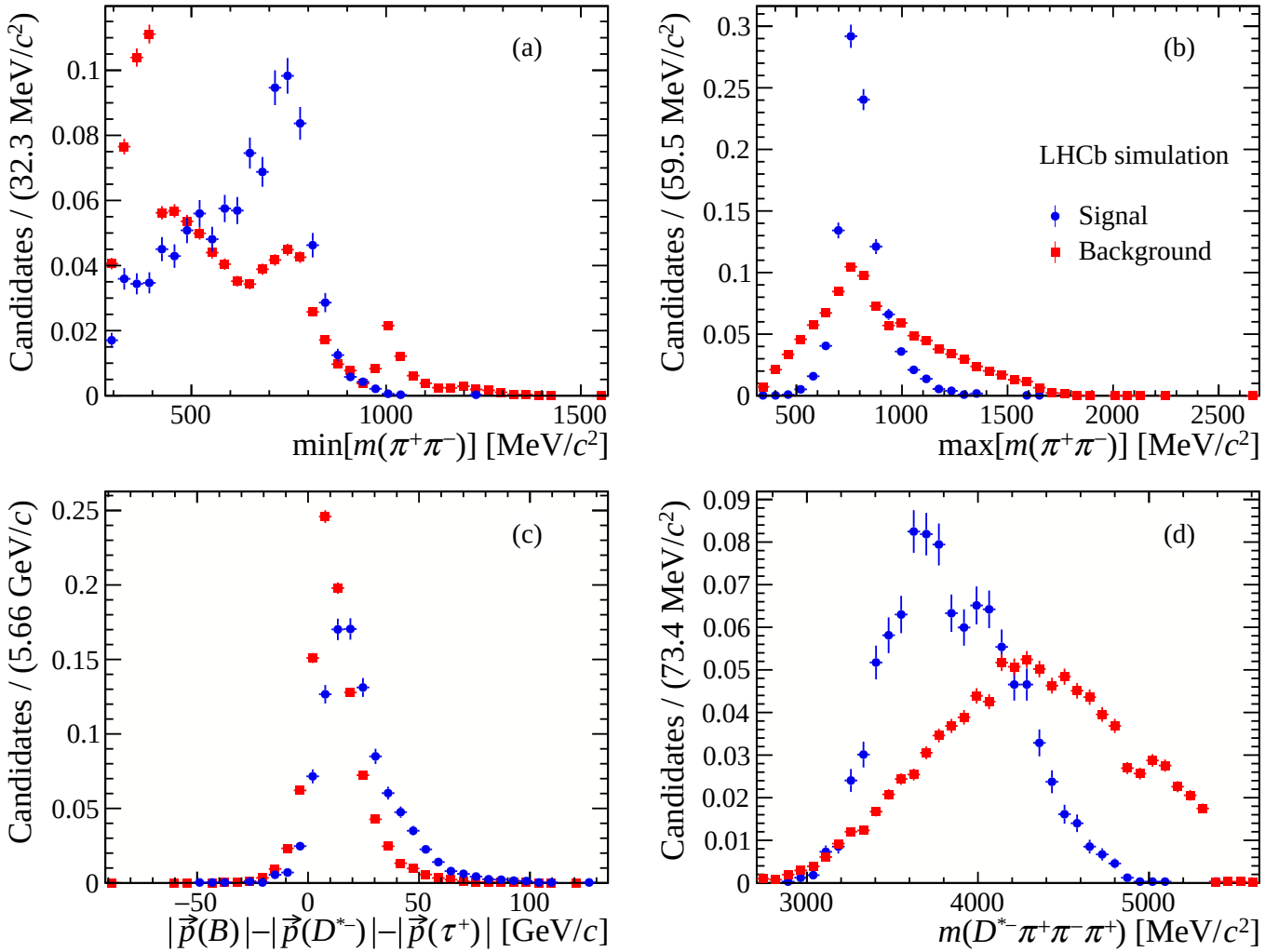

Normalized distributions of (a) min[$m(\pi^+\pi^-)$], (b) max[$m(\pi^+\pi^-)$], (c) approximated neutrino momentum reconstructed in the signal hypothesis, and (d) the $D^{*-}3\pi$ mass in simulated samples.

$R(D^*)$ hadronic ($\tau \to 3\pi\nu_\tau$) [PRD 97,072013 2018]

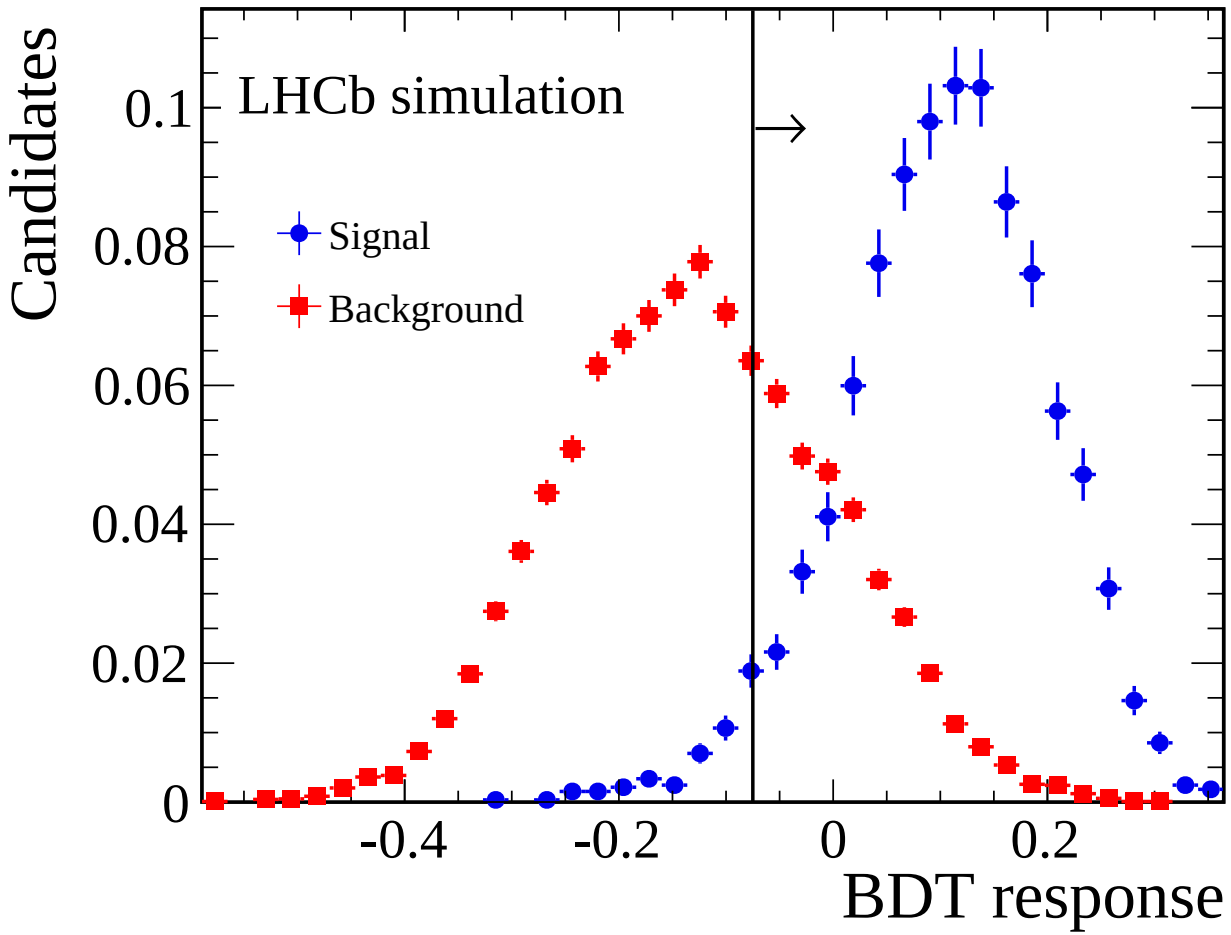

Distribution of the BDT response on the signal and background simulated samples.

$R(D^*)$ hadronic ($\tau \to 3\pi\nu_\tau$)
D_s^+, D^0 and D^+ control channels [PRD 97,072013 2018]

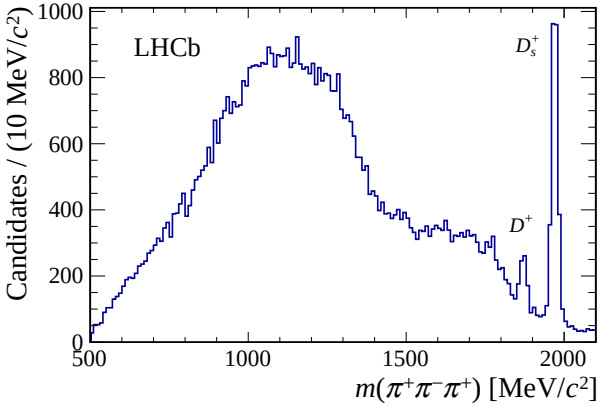

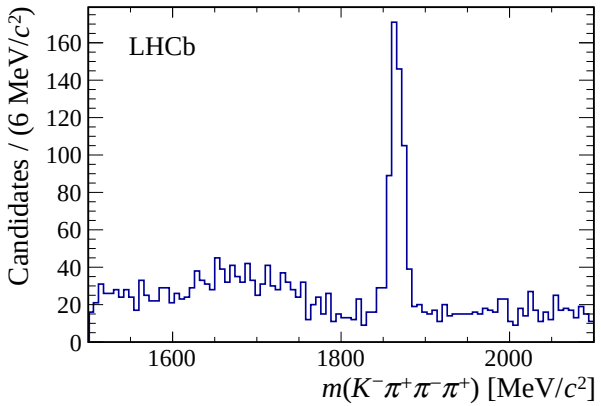

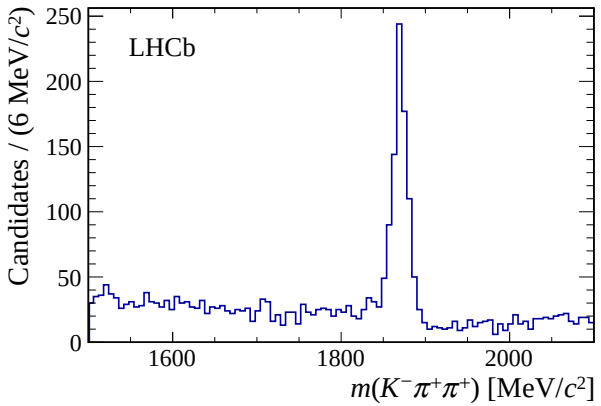

Left: Distribution of the 3π mass for candidates after the detached-vertex requirement. The D^+ and D_s^+ mass peaks are indicated.

Center: Distribution of the $K^-3\pi$ mass for D^0 candidates where a charged kaon has been associated to the 3π vertex. (anti-isolation)

Right: Distribution of the K^- π^+ π^+ mass for D^+ candidates passing the signal selection, where the negative pion has been identified as a kaon and assigned the kaon mass. (antiPID)

$R(D^*)$ hadronic ($\tau \to 3\pi\nu_\tau$). Neutral Isolation [PRD 97,072013 2018]

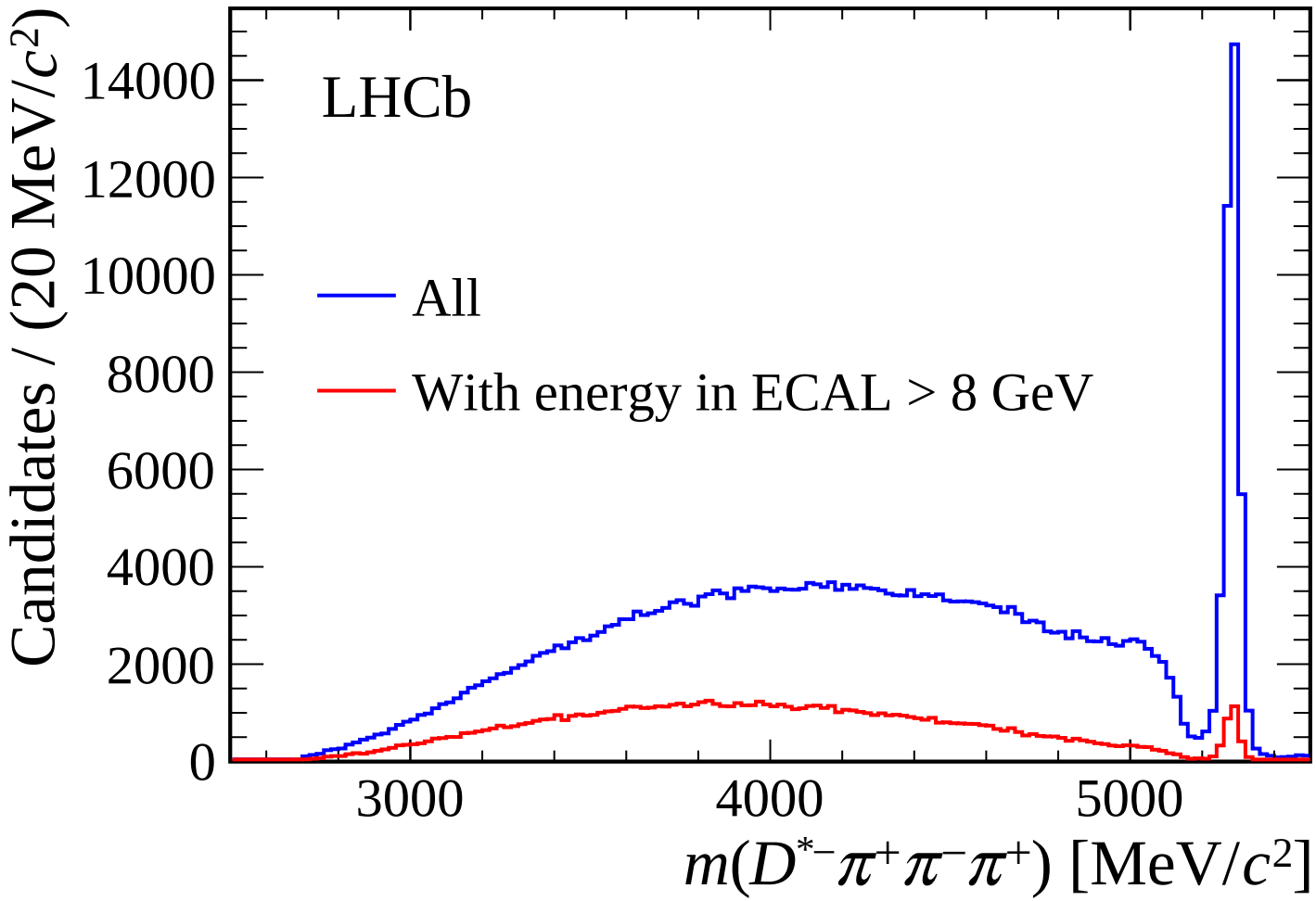

Distribution of the $D^{*-}3\pi$ mass (blue) before and (red) after a requirement of finding an energy of at least 8 GeV in the electromagnetic calorimeter around the 3π direction.

$R(D^*)$ hadronic ($\tau \to 3\pi\nu_\tau$) [PRD 97,072013 2018]

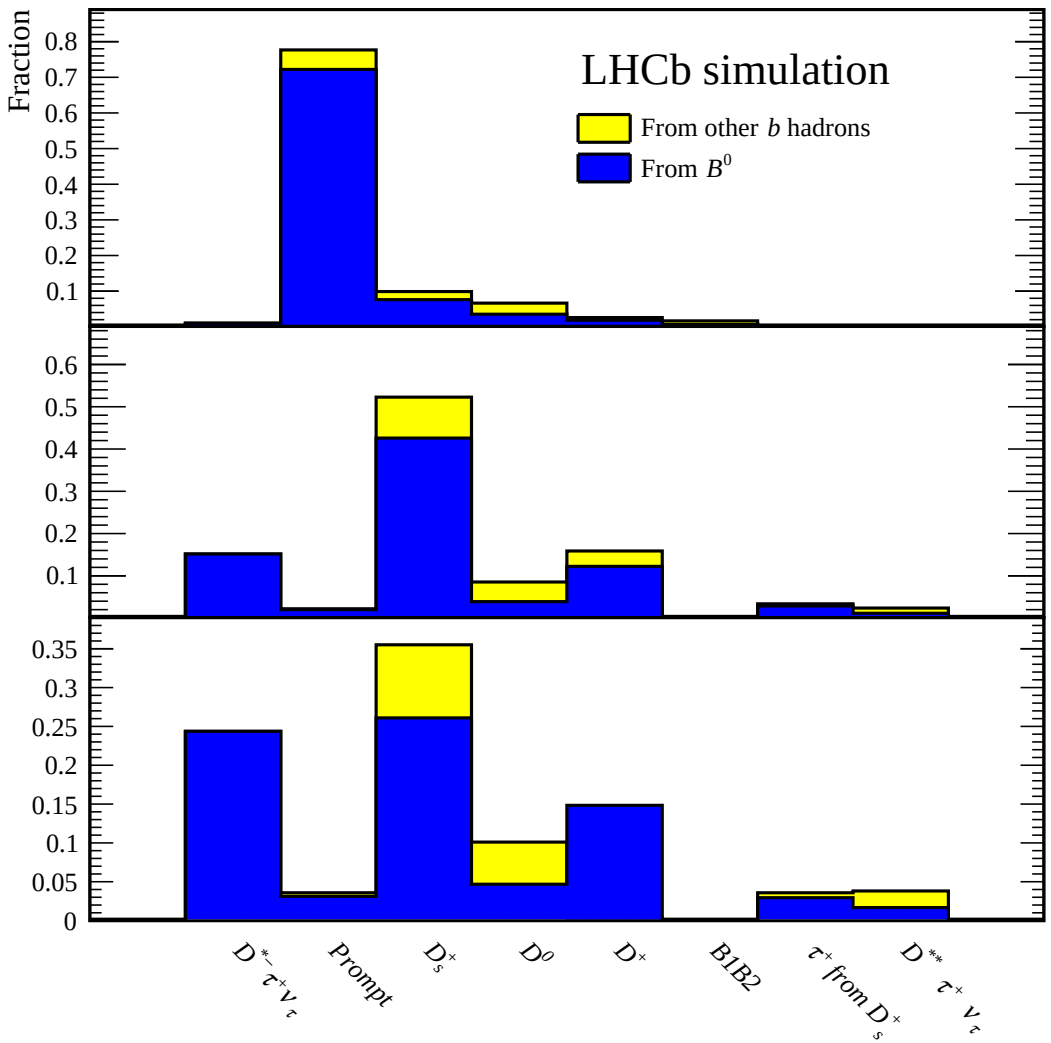

Composition of an inclusive simulated sample where a D^{*-} and a 3π system have been produced in the decay chain of a $b\bar{b}$ pair from a pp collision. Each bin shows the fractional contribution of the different possible parents of the 3π system (blue from a B^0, yellow for other b hadrons): from signal; directly from the b hadron (prompt); from a charm parent D_s^+, D^0, or D^+ meson; 3π from a B and the D^0 from the other B ($B1B2$); from τ lepton following a D_s^+ decay; from a τ lepton following a $D^{**}\tau^+\nu_\tau$ decay (D^{**} denotes here any higher excitation of D mesons).

(Top) After the initial selection and the removal of spurious 3π candidates.

(Middle) For candidates entering the signal fit.

(Bottom) For candidates populating the last 3 bins of the BDT distribution.

$R(D^*)$ hadronic ($\tau \to 3\pi\nu_\tau$) Control Sample [PRD 97,072013 2018]

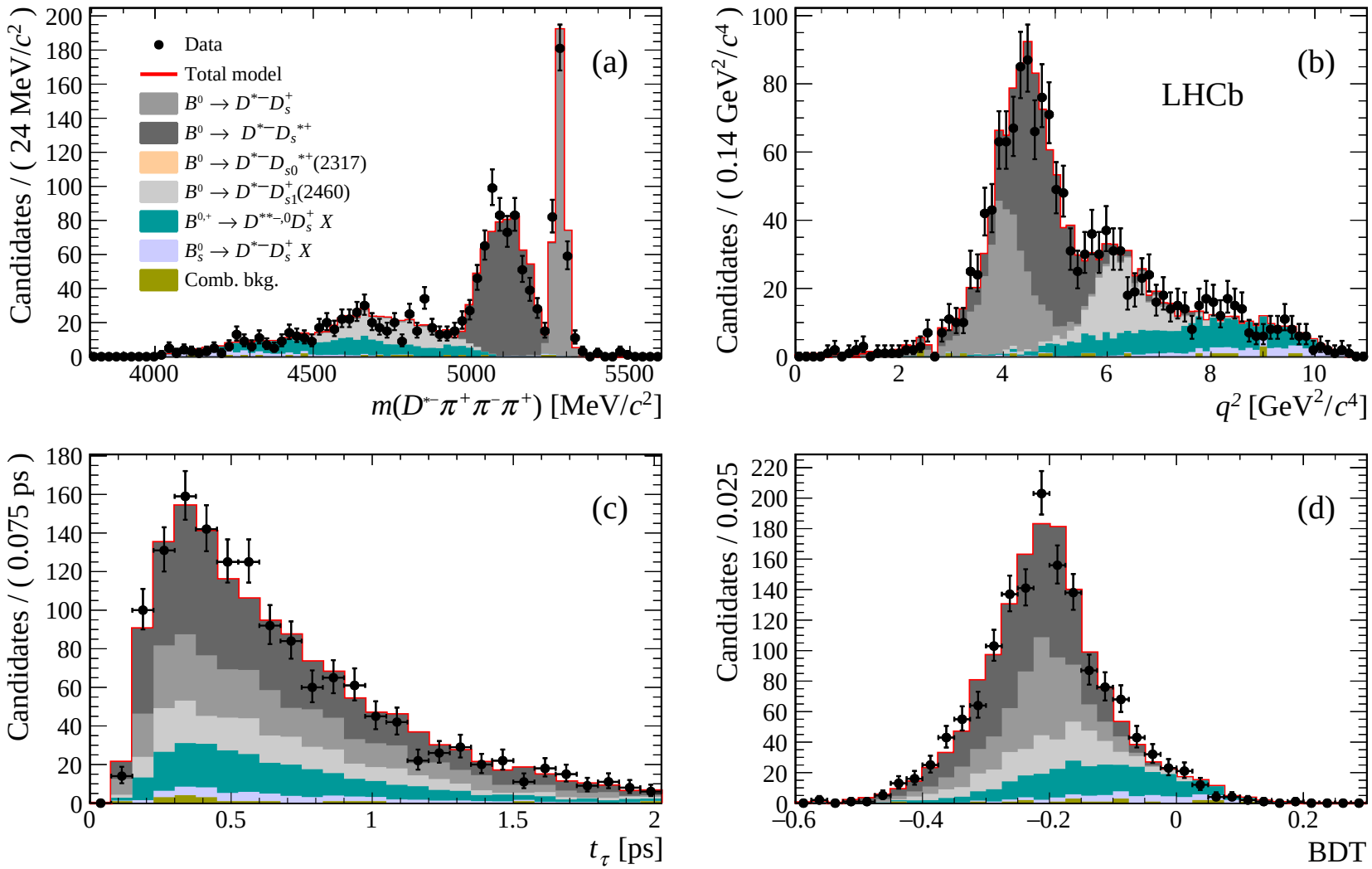

Results from the fit to data for candidates containing a $D^{*-} D_s^+$ pair, where $D_s^+ \to 3\pi$. The figures correspond to the fit projection on (a) $m(D^{*-}3\pi)$, (b) q^2, (c) 3π decaytime t_τ and(d) BDT output distributions.

$R(D^*)$ hadronic ($\tau \to 3\pi\nu_\tau$). D_s^+ decay model [PRD 97,072013 2018]

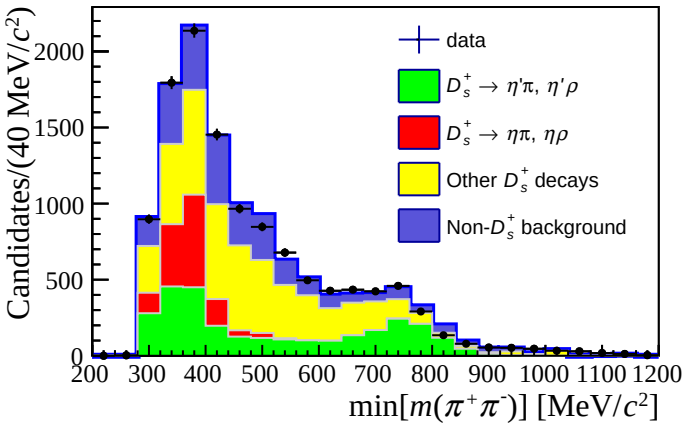

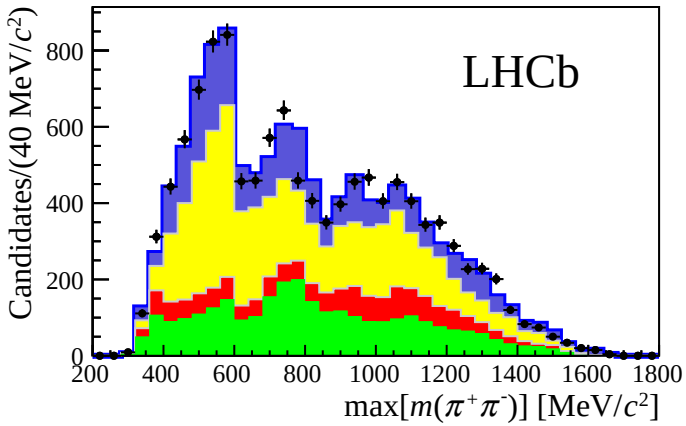

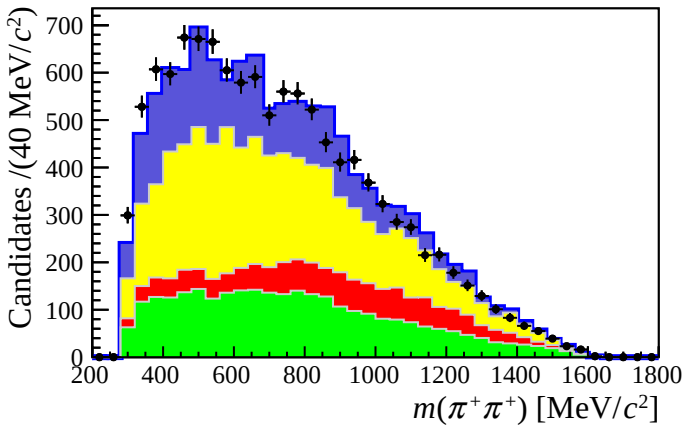

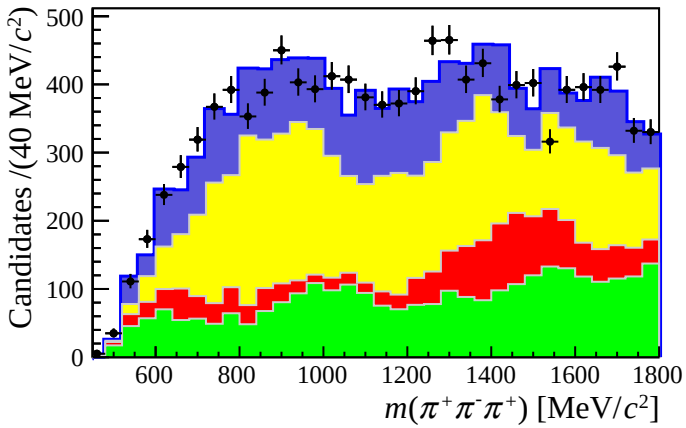

The 4 distributions are fitted simultaneously with a fit model obtained from MC. Sample enriched in $B \to D^{*-} D_s^+ (X)$ decays, obtained by requiring the BDT output below a certain threshold.

D_s^+ decays with at least 1 pion from η (red) or η' (green): $\eta^{(\prime)}\pi^+$, $\eta^{(\prime)}\rho^+$

D_s^+ decays with at least 1 pion from an intermediate state (IS) other than η or η': ω or ϕ (yellow)

D_s^+ decays where none of the 3 pions come from an IS, backgrounds originating from decays not involving the D_s^+ meson: $K^0 3\pi$, $\eta 3\pi$, $\eta' 3\pi$, $\omega 3\pi$, $\phi 3\pi$, non-resonnnt (blue).

$R(D^*)$ hadronic ($\tau \to 3\pi\nu_\tau$). D_s^+ decay model [PRD 97,072013 2018]

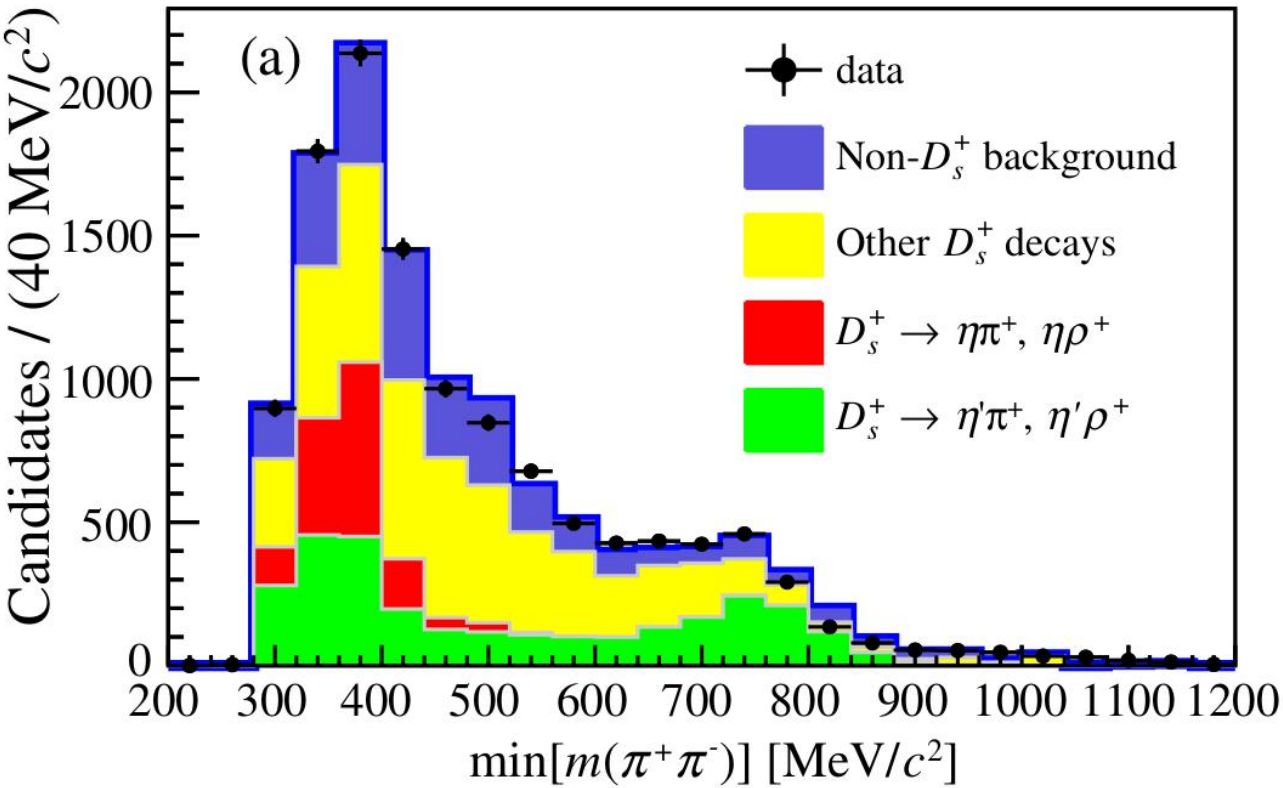

The τ lepton decays through the $a_1(1260)^+$ resonance, which leads to the $\rho^0\pi^+$ final. The dominant source of ρ^0 resonances in D_s^+ decays is due to $\eta' \to \rho^0\gamma$ decays. It is therefore crucial to control the η' contribution in D_s^+ decays very accurately.

At low min[$m(\pi^+\pi^-)$], only η and η' (red, green) contributions are peaking: $\eta \to \pi^+\pi^-\pi^0$ and $\eta' \to \eta\pi^+\pi^-$. At the ρ^0 mass where the signal lives, only η' contributes: $\eta' \to \rho^0\gamma$. The shape of this η' contribution is precisely known since the η' branching fractions are known to better than 2%. The precise measurement on data of the low-mass excess, which consists only of η' and η candidates, therefore enables the control of the η' contribution in the sensitive ρ region.

Fits results used to describe the $D_s^+ \to 3\pi X$ model in the final fit for $N_{\rm sig}$

$R(D^*)$ hadronic ($\tau \to 3\pi\nu_\tau$). D_s^+ decay model [PRD 97,072013 2018]

Results of the fit to the D_s^+ decay model. The relative contribution of each decay and the correction to be applied to the simulation are reported in the second and third columns, respectively.

D_s^+ decay	Relative contribution	Correction to simulation
$\eta\pi^+(X)$	0.156 ± 0.010	
$\eta\rho^+$	0.109 ± 0.016	0.88 ± 0.13
$\eta\pi^+$	0.047 ± 0.014	0.75 ± 0.23
$\eta'\pi^+(X)$	0.317 ± 0.015	
$\eta'\rho^+$	0.179 ± 0.016	0.710 ± 0.063
$\eta'\pi^+$	0.138 ± 0.015	0.808 ± 0.088
$\phi\pi^+(X)$, $\omega\pi^+(X)$	0.206 ± 0.02	
$\phi\rho^+$, $\omega\rho^+$	0.043 ± 0.022	0.28 ± 0.14
$\phi\pi^+$, $\omega\pi^+$	0.163 ± 0.021	1.588 ± 0.208
$\eta 3\pi$	0.104 ± 0.021	1.81 ± 0.36
$\eta' 3\pi$	0.0835 ± 0.0102	5.39 ± 0.66
$\omega 3\pi$	0.0415 ± 0.0122	5.19 ± 1.53
$K^0 3\pi$	0.0204 ± 0.0139	1.0 ± 0.7
$\phi 3\pi$	0.0141	0.97
$\tau^+(\to 3\pi(N)\overline{\nu}_\tau)\nu_\tau$	0.0135	0.97
$X_{\rm nr} 3\pi$	0.038 ± 0.005	6.69 ± 0.94

$R(D^*)$ hadronic ($\tau \to 3\pi\nu_\tau$) [PRD 97,072013 2018]

Projections of the three-dimensional fit on the
(a) 3π decay time
(b) q^2 and
(c) BDT output distributions.

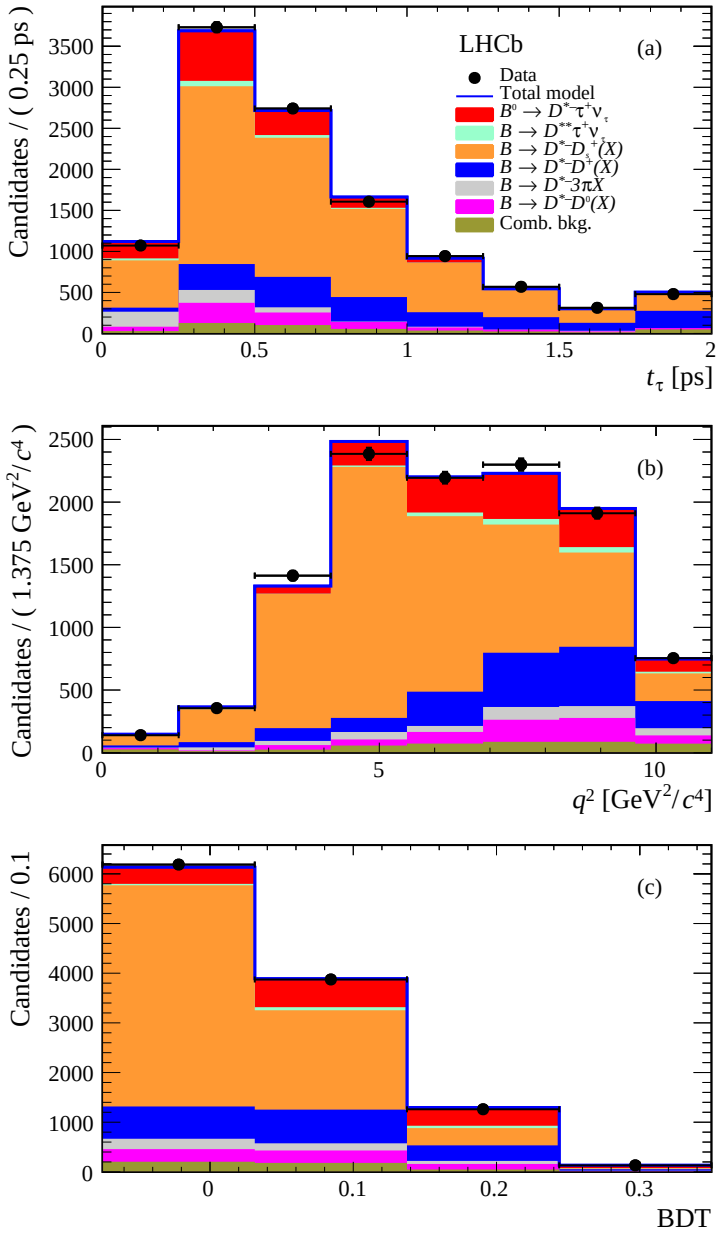

$R(D^*)$ hadronic ($\tau \to 3\pi\nu_\tau$) [PRD 97,072013 2018]

Summary of fit components and their corresponding normalization parameters. The first three components correspond to parameters related to the signal.

Fit component	Normalization
$B^0 \to D^{*-}\tau^+(\to 3\pi\overline{\nu}_\tau)\nu_\tau$	$N_{\rm sig} \times f_{\tau\to 3\pi\nu}$
$B^0 \to D^{*-}\tau^+(\to 3\pi\pi^0\overline{\nu}_\tau)\nu_\tau$	$N_{\rm sig} \times (1 - f_{\tau\to 3\pi\nu})$
$B \to D^{**}\tau^+\nu_\tau$	$N_{\rm sig} \times f_{D^{**}\tau\nu}$
$B \to D^{*-}D^+X$	$f_{D^+} \times N_{D_s}$
$B \to D^{*-}D^0X$ different vertices	$f^{v_1 v_2}_{D^0} \times N^{\rm sv}_{D^0}$
$B \to D^{*-}D^0X$ same vertex	$N^{\rm sv}_{D^0}$
$B^0 \to D^{*-}D_s^+$	$N_{D_s} \times f_{D_s^+}/k$
$B^0 \to D^{*-}D_s^{*+}$	$N_{D_s} \times 1/k$
$B^0 \to D^{*-}D^*_{s0}(2317)^+$	$N_{D_s} \times f_{D^{*+}_{s0}}/k$
$B^0 \to D^{*-}D_{s1}(2460)^+$	$N_{D_s} \times f_{D^+_{s1}}/k$
$B^{0,+} \to D^{**}D_s^+X$	$N_{D_s} \times f_{D_s^+X}/k$
$B_s^0 \to D^{*-}D_s^+X$	$N_{D_s} \times f_{(D_s^+X)_s}/k$
$B \to D^{*-}3\pi X$	$N_{B\to D^*3\pi X}$
B1B2 combinatorics	N_{B1B2}
Combinatoric D^{*-}	$N_{{\rm not}D^*}$

$R(D^*)$ hadronic ($\tau \to 3\pi\nu_\tau$) [PRD 97,072013 2018]

Fit results for the three-dimensional fit. The constraints on the parameters $f_{D_s^+}$, $f_{D_{s0}^{*+}}$, $f_{D_{s1}^+}$, $f_{D_s^+ X}$ and $f_{(D_s^+ X)_s}$ are applied taking into account their correlations.

Parameter	Fit result	Constraint
$N_{\rm sig}$	1296 ± 86	
$f_{\tau \to 3\pi\nu}$	0.78	0.78 (fixed)
$f_{D^{**}\tau\nu}$	0.11	0.11 (fixed)
$N^{\rm sv}_{D^0}$	445 ± 22	445 ± 22
$f^{\nu_1\nu_2}_{D^0}$	0.41 ± 0.22	
N_{D_s}	6835 ± 166	
f_{D^+}	0.245 ± 0.020	
$N_{B\to D^* 3\pi X}$	424 ± 21	443 ± 22
$f_{D_s^+}$	0.494 ± 0.028	0.467 ± 0.032
$f_{D_{s0}^{*+}}$	$0^{+0.010}_{-0.000}$	$0^{+0.042}_{-0.000}$
$f_{D_{s1}^+}$	0.384 ± 0.044	0.444 ± 0.064
$f_{D_s^+ X}$	0.836 ± 0.077	0.647 ± 0.107
$f_{(D_s^+ X)_s}$	0.159 ± 0.034	0.138 ± 0.040
N_{B1B2}	197	197 (fixed)
$N_{{\rm not}D^*}$	243	243 (fixed)

$R(D^*)$ hadronic ($\tau \to 3\pi\nu_\tau$) [PRD 97,072013 2018]

$$R(D^*) = 0.291 \pm 0.019(\text{stat}) \pm 0.026(\text{syst}) \pm 0.013(\text{ext})$$

List of the individual systematic uncertainties for $R(D^*)$:

Contribution	Value in %
$\mathcal{B}(\tau^+ \to 3\pi\overline{\nu}_\tau)/\mathcal{B}(\tau^+ \to 3\pi(\pi^0)\overline{\nu}_\tau)$	0.7
Form factors (template shapes)	0.7
Form factors (efficiency)	1.0
τ polarization effects	0.4
Other τ decays	1.0
$B \to D^{**}\tau^+\nu_\tau$	2.3
$B_s^0 \to D_s^{**}\tau^+\nu_\tau$ feed-down	1.5
$D_s^+ \to 3\pi X$ decay model	2.5
D_s^+, D^0 and D^+ template shape	2.9
$B \to D^{*-} D_s^+(X)$ and $B \to D^{*-} D^0(X)$ decay model	2.6
$D^{*-} 3\pi X$ from B decays	2.8
Combinatorial background (shape + normalization)	0.7
Bias due to empty bins in templates	1.3
Size of simulation samples	4.1
Trigger acceptance	1.2
Trigger efficiency	1.0
Online selection	2.0
Offline selection	2.0
Charged-isolation algorithm	1.0
Particle identification	1.3
Normalization channel	1.0
Signal efficiencies (size of simulation samples)	1.7
Normalization channel efficiency (size of simulation samples)	1.6
Normalization channel efficiency (modeling of $B^0 \to D^{*-} 3\pi$)	2.0
Total uncertainty	9.1

$R(D^*)$ hadronic ($\tau \to 3\pi\nu_\tau$) D^{**} [PRD 97,072013 2018]

- $B^0 \to D^{**}\tau\nu$ and $B^+ \to D^{**}\tau\nu$ constitute potential feed-down to the signal
- $D^{**}(2420)^0$ is reconstructed using its decay to $D^{*+}\pi^+$ **as a cross-check**
- The observation of the $D^{**}(2420)^0$ peak allows to compute the $D^{**}3\pi$ BDT distribution and to deduce a $D^{**}\tau\nu$ upper limit with the following assumption:
  - $D^{**0}\tau\nu = D^{**}(2420)^0\tau\nu$ (no sign of $D^{**}(2460)^0$)
  - $D^{**+}\tau\nu = D^{**0}\tau\nu$
- This upper limit is consistent with the theoretical prediction
- Subtraction in the signal of 0.11 ± 0.04 due to $D^{**}\tau\nu$ events leading to an error of 2.3%

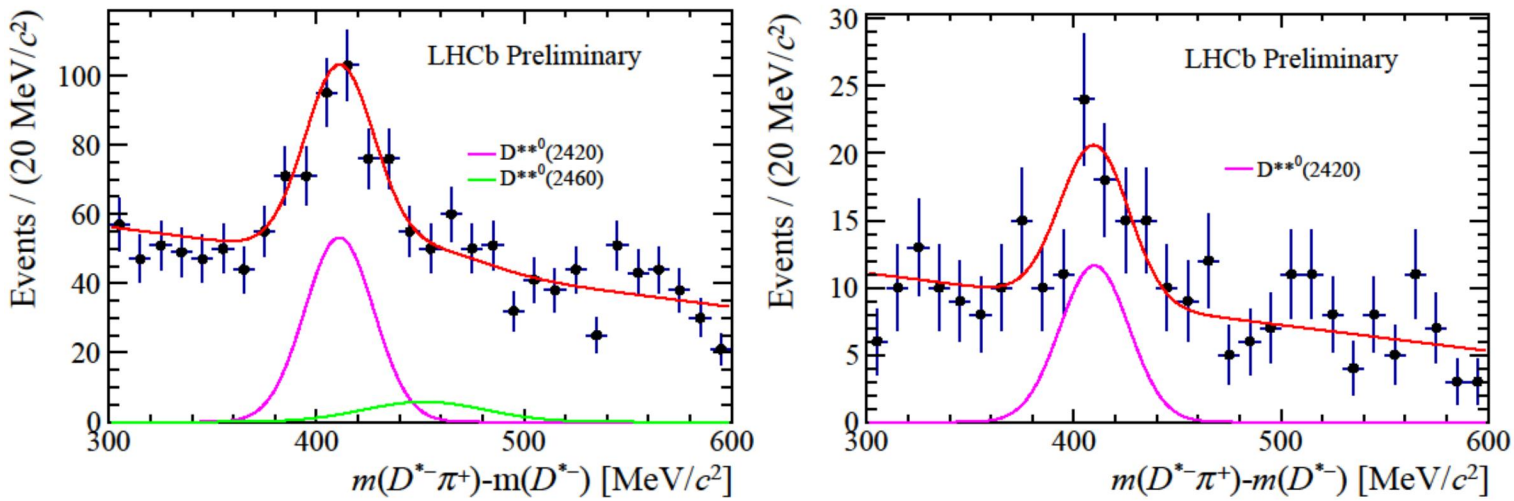

$R(D^*)$ hadronic ($\tau \to 3\pi\nu_\tau$) Systematics [PRL 120, 171802 2018]

$$R(D^*) = 0.291 \pm 0.019(\text{stat}) \pm 0.026(\text{syst}) \pm 0.013(\text{ext})$$

Breakdown of relative uncertainties:

Source	$\frac{\delta R(D^{*-})}{R(D^{*-})}$ [%]	Future
Simulated sample size	4.7	Produce more MC !
Empty bins in templates	1.3	
Signal decay model	1.8	
$D^{**}\ \tau\ \nu$ and $D_s^{**}\ \tau\ \nu$ feed-downs	2.7	Measure $R(D^{**}(2420)^0)$
$D_s^+ \to 3\pi X$ decay model	2.5	BESIII
$B \to D^{*-} D_s^+ X,\ D^{*-} D^+ X,\ D^{*-} D^0 X$ bkgs	3.9	Improves with stat
Combinatorial background	0.7	
$B \to D^{*-} 3\pi X$ background	2.8	Kill with $\lvert z\tau - zD\rvert > 5\sigma$
Efficiency ratio	3.9	Improves with stat
Normalization channel efficiency (modeling of $B^0 \to D^{*-} 3\pi$)	2.0	
Total systematic uncertainty	9.1	
Statistical uncertainty	6.5	
Total uncertainty	11.9	

$R(D^*)$ hadronic ($\tau \to 3\pi\nu_\tau$) Improvement of systematics in the future [PRL 120, 171802 2018]

$$R(D^*) = 0.291 \pm 0.019(\text{stat}) \pm 0.026(\text{syst}) \pm 0.013(\text{ext})$$

- Shape of $B \to D^* DX$ background (2.9%): scale with statistics
- $D_s^+ \to 3\pi X$ decay model (2.5%): BESIII future measurement will help to significantly reduce this uncertainty.
- Branching fraction of normalisation mode $B^0 \to D^* 3\pi$ can be precisely measured by Belle II.
- $B \to D^{*-} 3\pi X$ background can be easily removed by a strong cut on the distance significance between the τ and the D^0 vertices.
- With more stat, measure $R(D^{**}(2420)^0)$ and constraint D^{**} feed-down
- Efficiency ratio: will improve with more stat.

$B_c^+ \to J/\psi \tau^+ \nu : R_{J/\psi}$

$B_c^+ \to J/\psi \tau^+ \nu$: $R_{J/\psi}$ [PRL 120, 121801 (2018)]

- Generalization of $R(D^*)$ to B_c^+

$$R(J/\psi) = \frac{\mathcal{B}(B_c^+ \to J/\psi \tau^+ \nu_\tau)}{\mathcal{B}(B_c^+ \to J/\psi \mu^+ \nu_\mu)}$$

- B_c^+ decay form factors unconstrained experimentally: theoretical prediction not yet precise 0.25-0.28
- Reconstruct signal with $\tau \to \mu \nu_\mu \nu_\tau$ (17%)
- Like in $R(D^*)$, use m^2_{miss}, E^*_μ and q^2. Add information from B_c^+ decay time
- Imperfect reconstruction due to missing neutrinos. The broad shapes of the distributions are smeared but their discriminating power is preserved

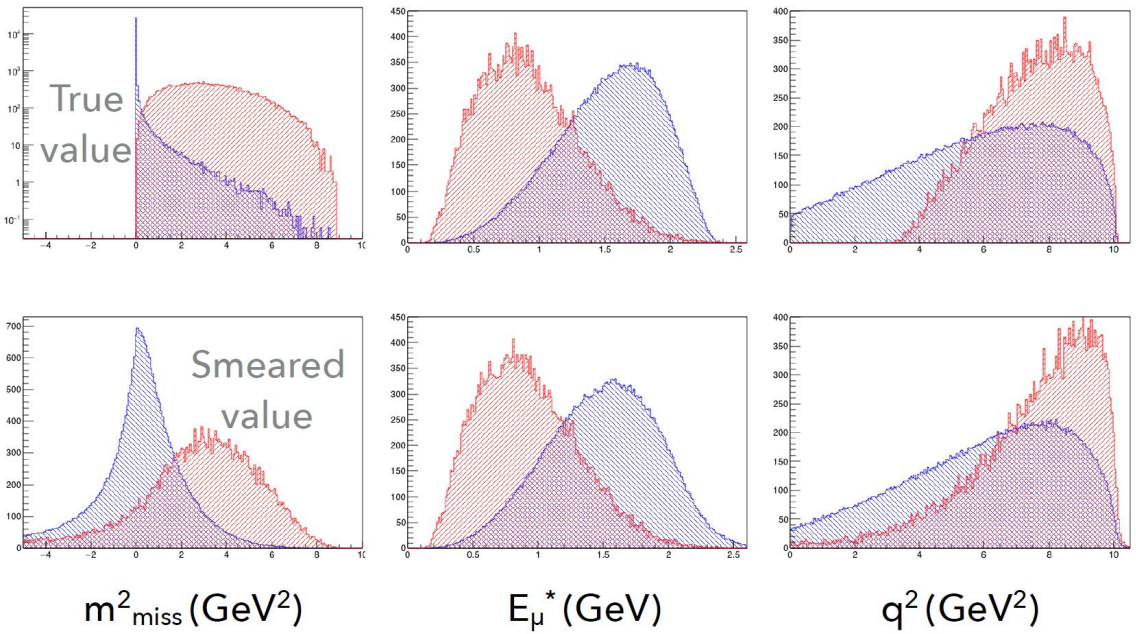

Systematic uncertainties

Model uncertainties	**Size (eff. corrected) ($\times 10^{-2}$)**
Uncertainty due to finite size of simulation data	8.0
$B_c^+ \to J/\psi$ form factors	12.1
$B_c^+ \to \psi(2S)$ form factors	3.2
Bias correction	5.4
$B_c^+ \to J/\psi H_c X$ cocktail composition	3.6
Z binning strategy	5.6
Misidentification background strategy	5.4
Combinatorial background cocktail	4.5
Combinatorial J/ψ sideband scaling	0.9
Empirical reweighting	1.6
Semitauonic $\psi(2S)$ and χ_c feed-down	0.9
Fixing $A_2(q^2)$ slope to zero	0.3
Efficiency ratio	0.6
$\mathcal{B}(\tau \to \mu\nu\nu)$	0.2
B_c^+ lifetime	included in stat.
Total systematic uncertainty	**17.7**
Statistical uncertainty	**17.3**

$B_c \to J/\psi\,\tau\nu$: $R_{J/\psi}$ [PRL 120, 121801 (2018)]

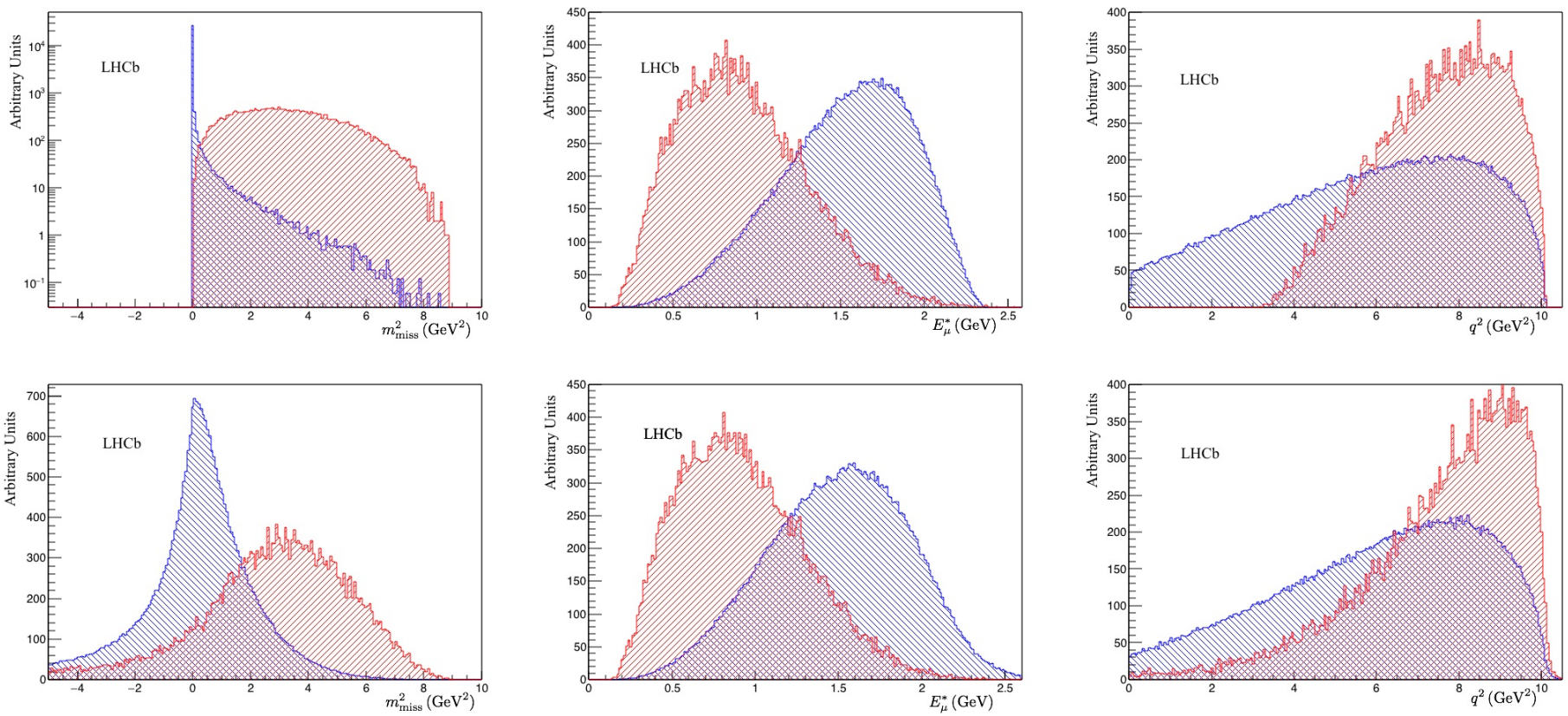

For each fit variable (save the mostly unaltered decay time), the distributions of the quantity calculated using the simulated true B_c^+ momentum and the approximated momentum are shown. In each plot, the normalization $B_c^+ \to J/\psi\,\mu^+\nu_\mu$ decay is shown in blue, while the signal $B_c^+ \to J/\psi\,\tau^+\nu_\tau$ is shown in red. The smearing induced by the rest frame approximation does not wash out the discriminating power of these variables.

Trick to make a 3D fit with 4 variables: the Z variable merges information from q^2 and E^*_μ

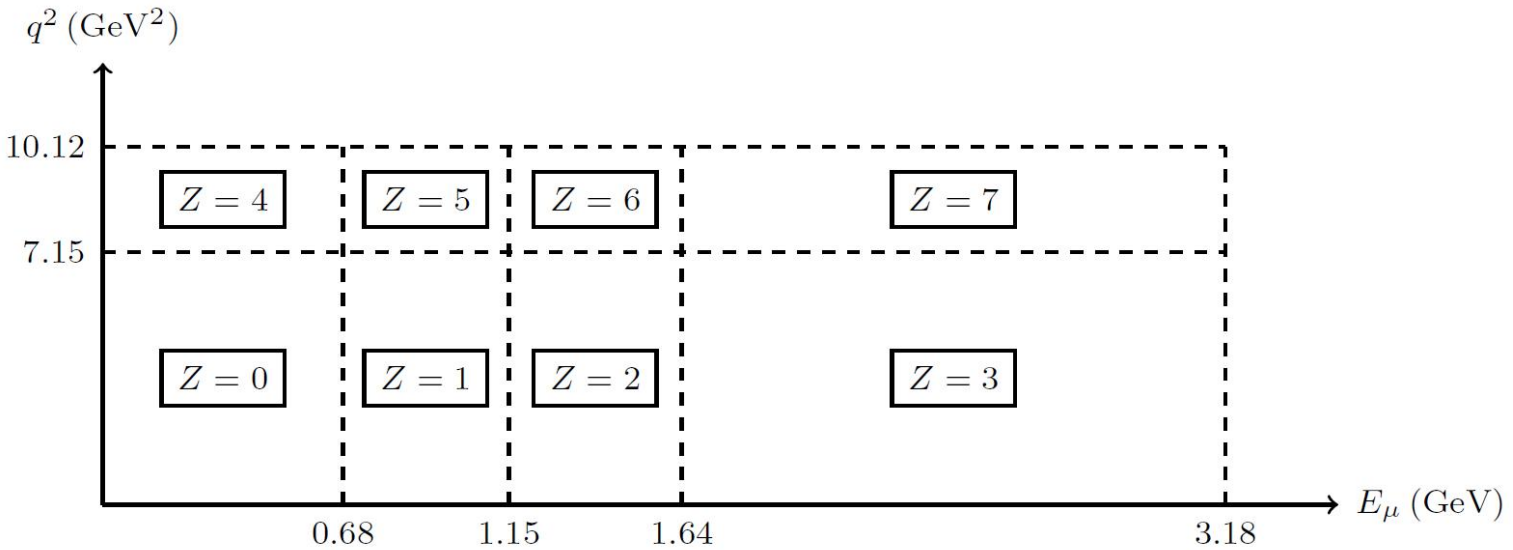

Charmonium feed-down background

- Virtually all the feed down comes from hadronic ψ(2S) and radiative χ_c(1P) decays
- Ignoring contributions of DD threshold (e.g. ψ(3770), X(3872), etc.) and assigning appropriate systematic uncertainties

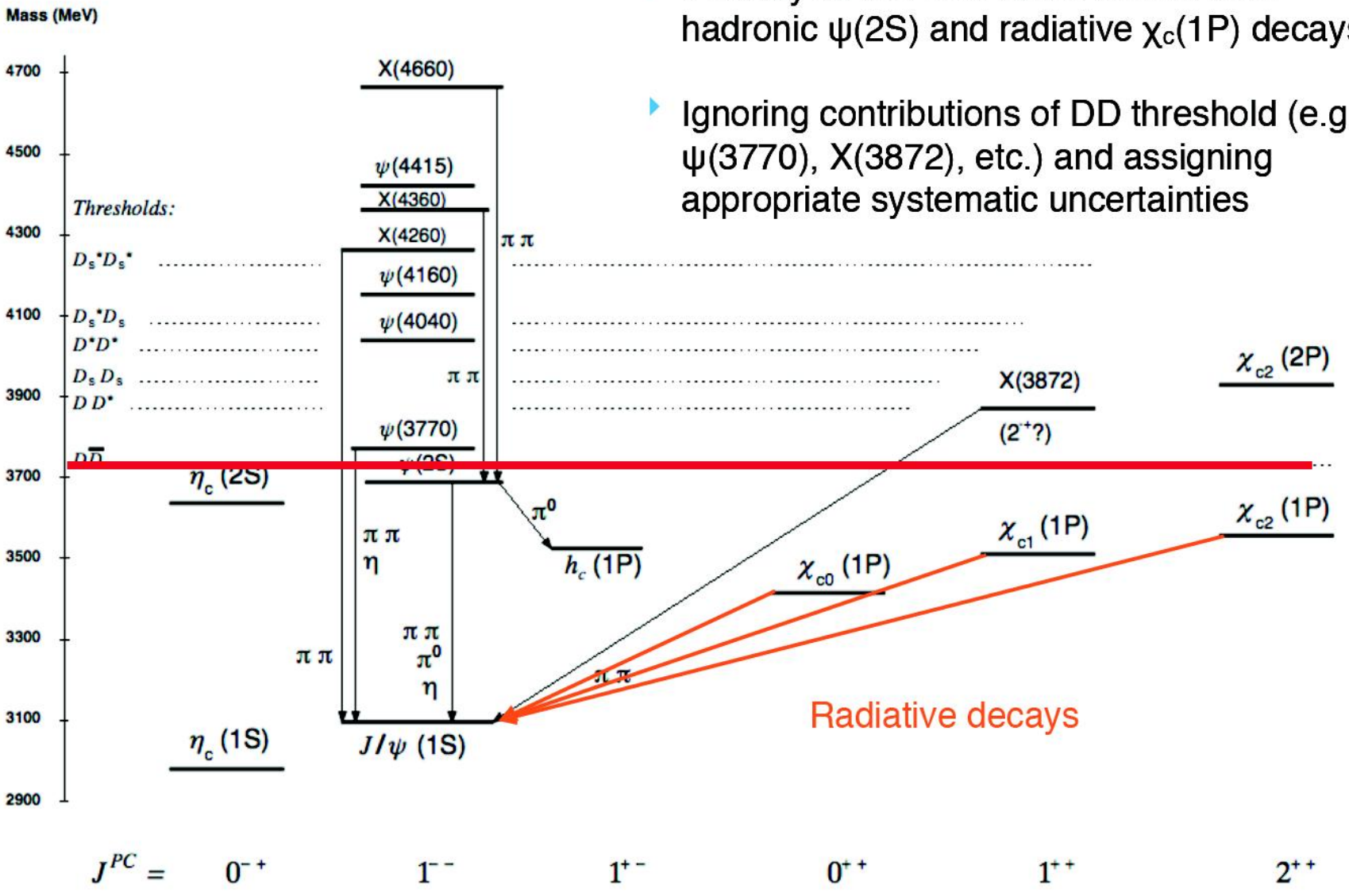

$B_c^+ \to J/\psi\,\tau\nu$: $R_{J/\psi}$ About the form factors [PRL 120, 121801 (2018)]

The templates are derived from simulation for the signal and the normalization modes, which requires knowledge of the $B_c^+ \to J/\psi\,\ell^+\nu_\ell$ form factors. These have not yet been precisely determined and the theoretical predictions, e.g. those from Kiselev, Ebert, Faustov, and Galkin have be tested against data. Thus, for this measurement, the shared form factors for the signal and normalization channels are determined directly from the data by employing a z-expansion parametrization inspired by [BCL] to fit a subsample of the data excluding events with missing mass greater than $1\,\mathrm{GeV}^2/c^4$. In this expansion, the form factor $V(q^2)$, $A_0(q^2)$, $A_1(q^2)$, and $A_2(q^2)$ (following the convention of [Ebert] are fit by functions of the form

$$f(q^2) = \frac{1}{1 - q^2/M_{\mathrm{pole}}^2} \sum_{k=0}^{K} a_k z(q^2)^k,$$

where $z(q^2)$ is defined in [BCL]. The pole mass M_{pole} is the mass of the excited B_c^+ state with quantum numbers corresponding to the form factor: the $J^P = 1^-$ state for $V(q^2)$, taken to be $6.33\,\mathrm{GeV}/c^2$; the 0^- state for $A_0(q^2)$, which is the B_c^+ mass itself; and finally the 1^+ state for $A_1(q^2)$ and $A_2(q^2)$, taken to be $6.73\,\mathrm{GeV}/c$ [Ebertz,Kiselev]. The form factor $A_0(q^2)$ is fit to $K = 0$ order, while the others are fit to the linear $K = 1$ order. The parameters obtained from this procedure contain the effects of the reconstruction resolution of the kinematic parameters and cannot be directly compared with existing theoretical predictions.

LHCb and future plans

LHCb: general-purpose detector in the forward region at the LHC [Int. J. Mod. Phys. A 30, 1530022 (2015)]

LHCb is a forward spectrometer installed on the LHC with a **broad physics program** continually expanding:

- CKM and CP violation in *b* and *c* hadrons
- Rare decays of *b* and *c* hadrons
- Heavy quark production
- Spectroscopy including tetraquarks, pentaquarks, ...
- Kaon physics
- Electroweak, QCD, exotica, ...
- Higgs and top
- Heavy ion physics (p-Pb, Pb-Pb), fixed-target collisions (He, Ne, Ar).

Examples of publications, well beyond *b*-physics:

[Search for Majorana neutrinos in $B^- \to \pi\mu^+\mu^+$ decays, PRL 2014],
[Search for dark photons produced in 13 TeV *pp* collision, PRL 2018],
[Measurement of forward top pair production in the dilepton channel in *pp* collisions at $\sqrt{s} = 13$ TeV, 1803.05188],
[Measurements of long-range near-side angular correlations in $\sqrt{s_{NN}} = 5$ TeV proton-lead collisions in the forward region, PLB 2016],
[Limits on neutral Higgs boson production in the forward region in pp collisions at $\sqrt{s} = 7$ TeV, JHEP 2013]

The LHCb detector [Int. J. Mod. Phys. A 30, 1530022 (2015)]

- Advantages:
  - Excellent vertexing, tracking and PID
  - Trigger also on low momentum hadrons
  - Enormous data sample from LHC high $b\bar{b}$ cross section
  - All type of b-hadrons, including B_c^+ and Λ_b

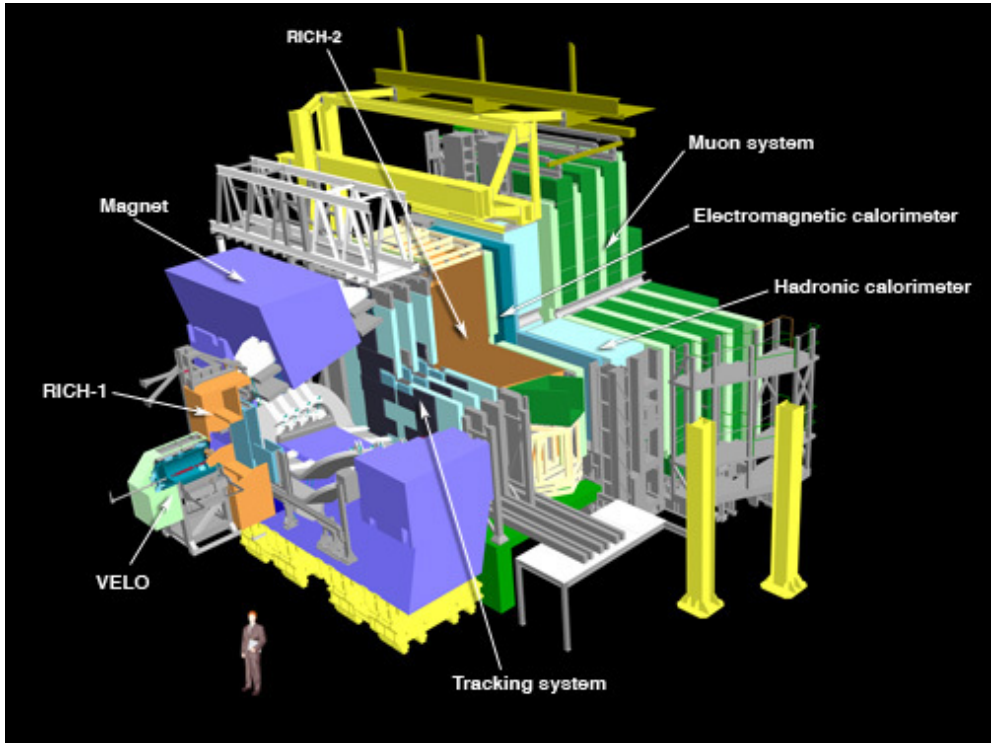

- Challenges:
  - Missing neutrinos $\rightarrow$ unconstrained kinematics
  - High track multiplicity $\rightarrow$ significant amount of background
  - High particle momenta $\rightarrow$ significant Bremsstrahlung for electrons

In this talk: ONLY Run 1 data, 3 fb^{-1}, 2011(12), $\sqrt{s} = 7(8)$ TeV

LHCb plans

- Run 2 (2016-2018): $6\,\text{fb}^{-1}$ at $\sqrt{s} = 13\,\text{TeV}$, improved trigger
- Some major experimental measurements (e.g. γ, $B_s^0 \to \phi\phi$) are not yet at the level of theoretical prediction
- Above a luminosity of $\sim 4 \times 10^{32}\text{cm}^{-2}\text{s}^{-1}$, LHCb efficiency to trigger hadronic modes saturates, because of the L0-trigger bottleneck which can not cope with more than 1 MHz output rate.

$\Rightarrow$ upgrade 1 of the LHCb experiment in 2019:

- Full software trigger: read all detector at 40 MHz $\to \times 2$ efficiency for hadronic final state.
- Luminosity up to $2 \times 10^{33}\text{cm}^{-2}\text{s}^{-1}$, new challenges: high pile-up, large occupancies, radiation damages
- Detector upgrades: VELO (pixels), tracker (Silicon strips and scintillating fibers), RICH (multi-anode PMTs), CALO& MUON (new electronics), ...
- Aim to collect $\sim$50 fb^{-1}. Annual yields wrt published analyses: $\times 10$ for muonic final states and $\times 20$ for hadronic modes.

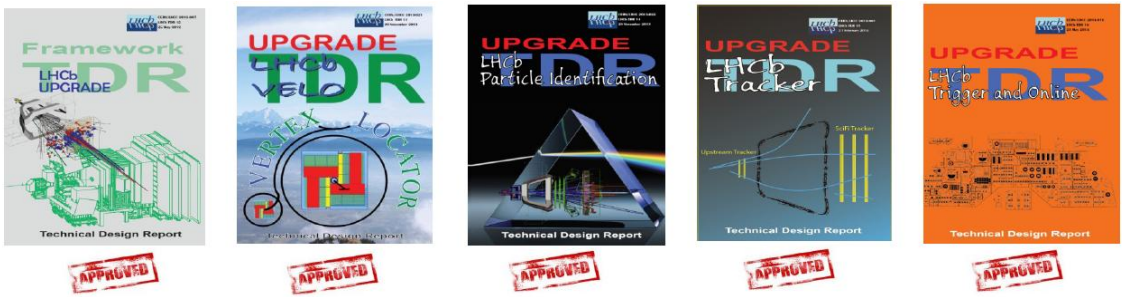

Expected performances of LHCb upgrade 1 [LHCb-PUB-2014-040]

Type	Observable	LHC Run 1	LHCb 2018	**LHCb upgrade**	Theory
B_s^0 mixing	$\phi_s(B_s^0 \to J/\psi\,\phi)$ (rad)	0.049	0.025	**0.009**	~ 0.003
	$\phi_s(B_s^0 \to J/\psi\, f_0(980))$ (rad)	0.068	0.035	**0.012**	~ 0.01
	$A_{\rm sl}(B_s^0)$ (10^{-3})	2.8	1.4	**0.5**	0.03
Gluonic	$\phi_s^{\rm eff}(B_s^0 \to \phi\phi)$ (rad)	0.15	0.10	**0.018**	0.02
penguin	$\phi_s^{\rm eff}(B_s^0 \to K^{*0}\bar{K}^{*0})$ (rad)	0.19	0.13	**0.023**	< 0.02
	$2\beta^{\rm eff}(B^0 \to \phi K_S^0)$ (rad)	0.30	0.20	**0.036**	0.02
Right-handed	$\phi_s^{\rm eff}(B_s^0 \to \phi\gamma)$ (rad)	0.20	0.13	**0.025**	< 0.01
currents	$\tau^{\rm eff}(B_s^0 \to \phi\gamma)/\tau_{B_s^0}$	5%	3.2%	**0.6%**	0.2 %
Electroweak	$S_3(B^0 \to K^{*0}\mu^+\mu^-; 1 < q^2 < 6\,{\rm GeV}^2/c^4)$	0.04	0.020	**0.007**	0.02
penguin	$q_0^2\, A_{\rm FB}(B^0 \to K^{*0}\mu^+\mu^-)$	10%	5%	**1.9%**	$\sim 7\%$
	$A_{\rm I}(K\mu^+\mu^-; 1 < q^2 < 6\,{\rm GeV}^2/c^4)$	0.09	0.05	**0.017**	~ 0.02
	$\mathcal{B}(B^+ \to \pi^+\mu^+\mu^-)/\mathcal{B}(B^+ \to K^+\mu^+\mu^-)$	14%	7%	**2.4%**	$\sim 10\%$
Higgs	$\mathcal{B}(B_s^0 \to \mu^+\mu^-)$ (10^{-9})	1.0	0.5	**0.19**	0.3
penguin	$\mathcal{B}(B^0 \to \mu^+\mu^-)/\mathcal{B}(B_s^0 \to \mu^+\mu^-)$	220%	110%	**40%**	$\sim 5\,\%$
Unitarity	$\gamma(B \to D^{(*)}K^{(*)})$	7°	4°	**0.9°**	negligible
triangle	$\gamma(B_s^0 \to D_s^{\mp}K^{\pm})$	17°	11°	**2.0°**	negligible
angles	$\beta(B^0 \to J/\psi\, K_S^0)$	1.7°	0.8°	**0.31°**	negligible
Charm	$A_\Gamma(D^0 \to K^+K^-)$ (10^{-4})	3.4	2.2	**0.4**	–
CP violation	ΔA_{CP} (10^{-3})	0.8	0.5	**0.1**	–

- $\phi_s^{\rm eff}(B_s^0 \to \phi\phi)$ with a precision of 0.018
- γ with a precision below 1°

Planning LHC 2035

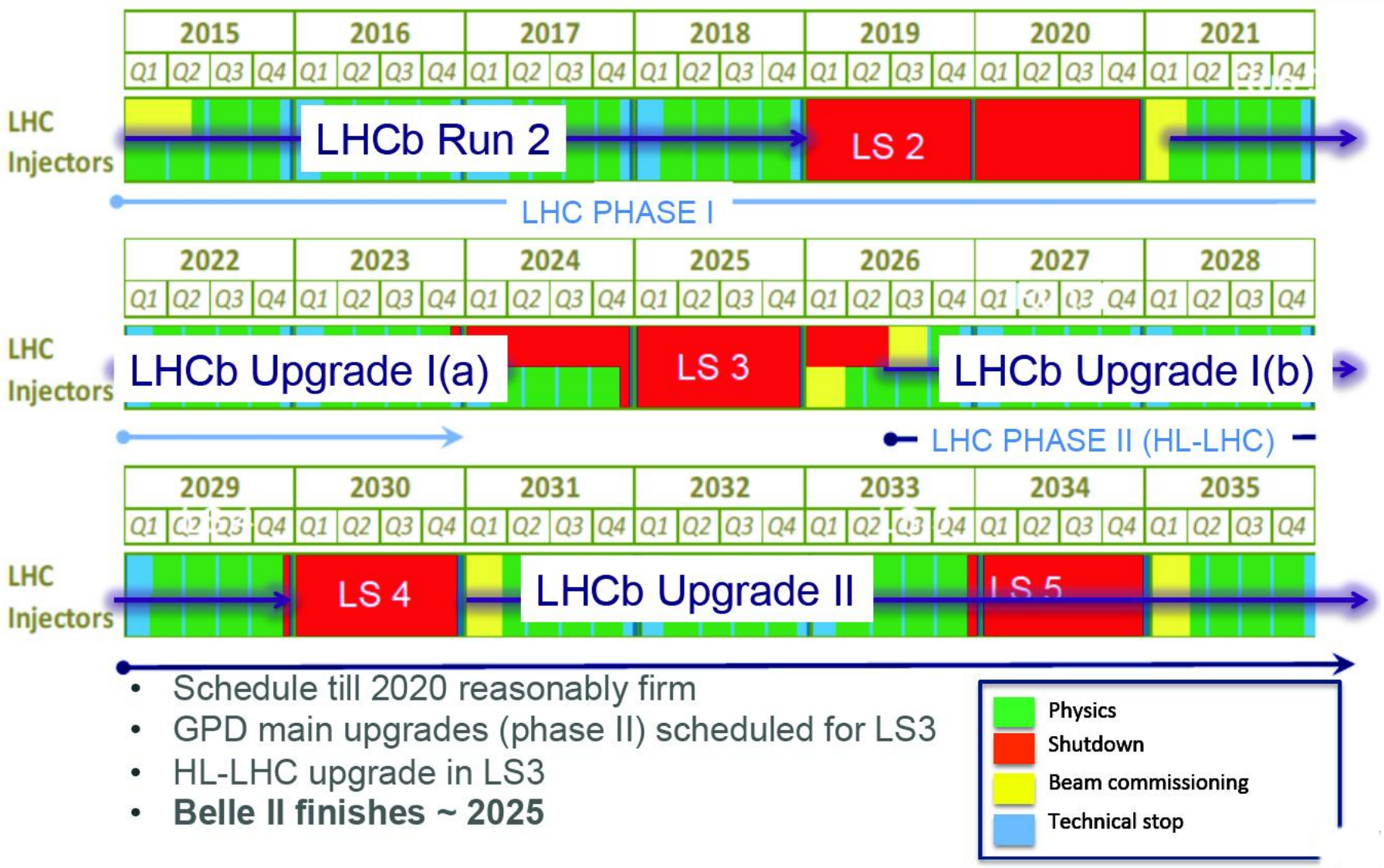

- Schedule till 2020 reasonably firm
- GPD main upgrades (phase II) scheduled for LS3
- HL-LHC upgrade in LS3
- **Belle II finishes ~ 2025**

Planning LHC 2035

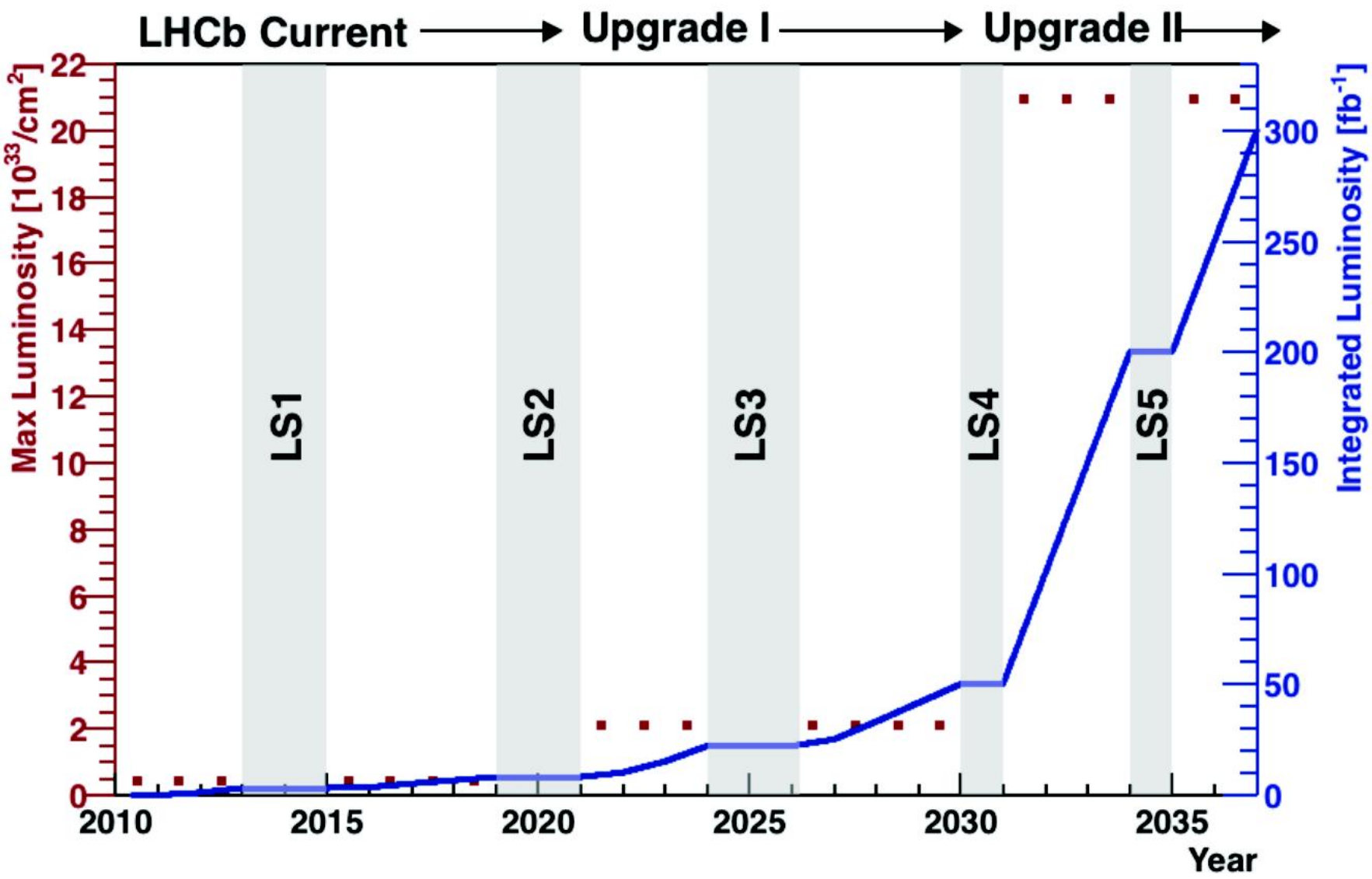

The LHCb detector [JINST 3 (2008 S08005)]

- Single-arm forward spectrometer:
  - Tracking system
    IP resolution $\sim 15\mu$m (at high p_{T})
    $\delta p/p \sim 0.45\%$
  - RICH system
    Very good $K - \pi$ identification for
    $p \sim 2 - 100\,\mathrm{GeV}/c$
  - Calorimeters
    Energy measurement, identify π^0,γ,e
    + trigger
  - Muon detector
    muon identification + trigger

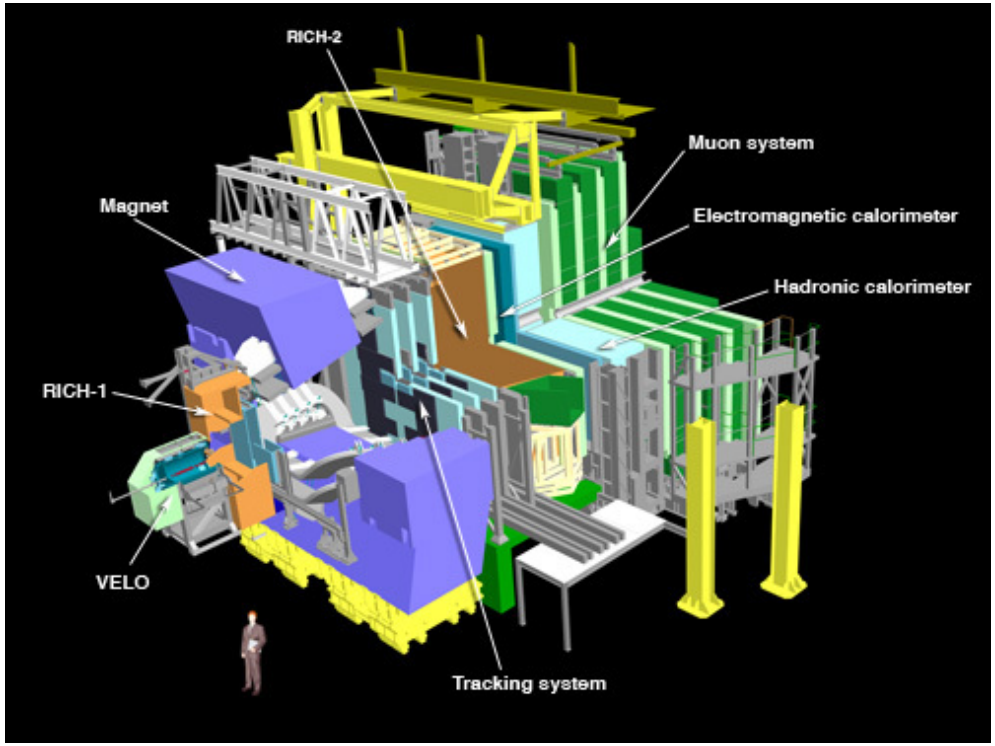

- Integrated lumi $1\,\mathrm{fb}^{-1}$ (2011), $2\,\mathrm{fb}^{-1}$ (2012)
  Instantaneous lumi $\sim 1 - 4 \times 10^{32}\mathrm{cm}^{-2}\mathrm{s}^{-1}$

LHCb: general-purpose detector at the LHC

LHCb is a forward spectrometer installed on the LHC, with a broad physics program, continually expanding:

- CKM and CP violation
- Rare decays
- Charm physics
- Kaon physics
- Spectroscopy in *pp* interactions
- Heavy quark production
- Exotica searches (tetraquarks, pentaquarks, dark sector, ...)
- Electroweak and QCD measurements in the forward region
- Higgs and top
- Heavy ion physics (p-Pb, Pb-Pb), fixed-target collisions (He, Ne, Ar).

Examples of publications, well beyond *b*-physics:

[Search for Majorana neutrinos in $B^- \to \pi \mu^+ \mu^+$ decays, PRL 2014],
[Search for dark photons produced in 13 TeV *pp* collision, PRL 2018],
[Measurement of forward top pair production in the dilepton channel in *pp* collisions at $\sqrt{s} = 13$ TeV, 1803.05188],
[Measurements of long-range near-side angular correlations in $\sqrt{s_{NN}} = 5$ TeV proton-lead collisions in the forward region, PLB 2016],
[Limits on neutral Higgs boson production in the forward region in pp collisions at $\sqrt{s} = 7$ TeV, JHEP 2013]

The LHCb Trigger in 2011–2012

- L0 hardware trigger:
  - Find lepton, hadron with high p_T
  - Reduce the rate from 40 MHz to 1 MHz
- HLT1 software trigger:
  - Finds vertices in VELO
  - Tracks with high IP & p_T
- HLT2 software trigger:
  - Reconstruct all tracks in event
  - Select inclusive/exclusive b-hadrons
  - Output rate = 5 kHz

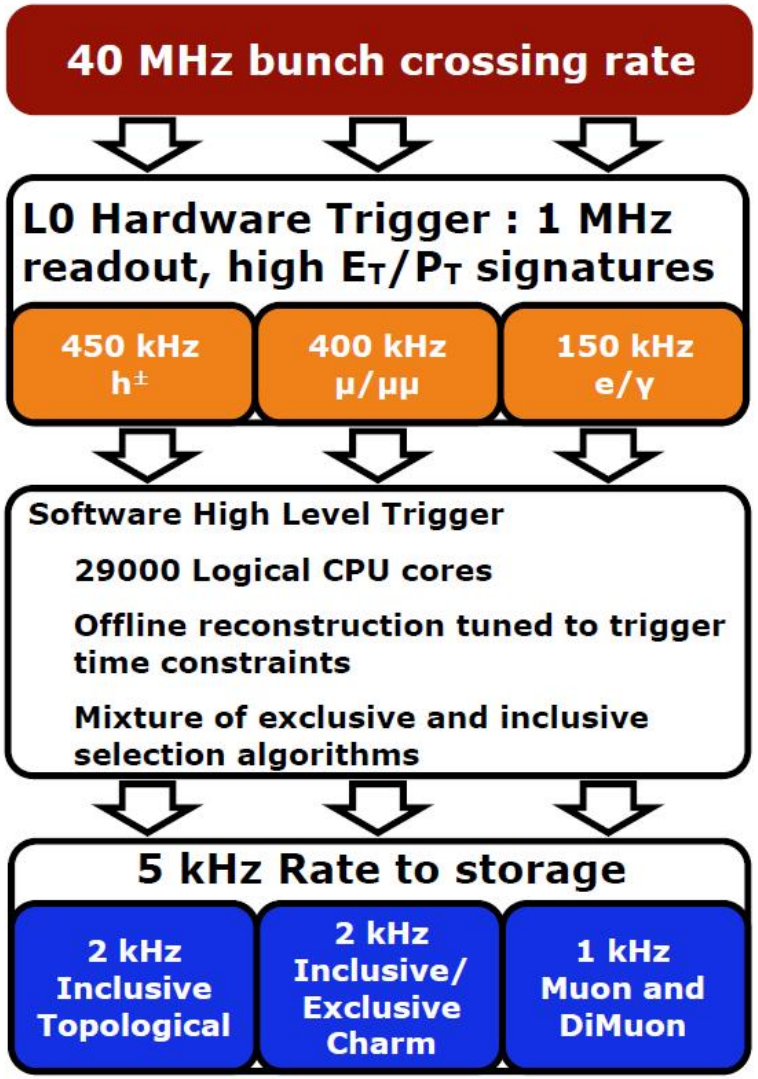

Trigger in 2015

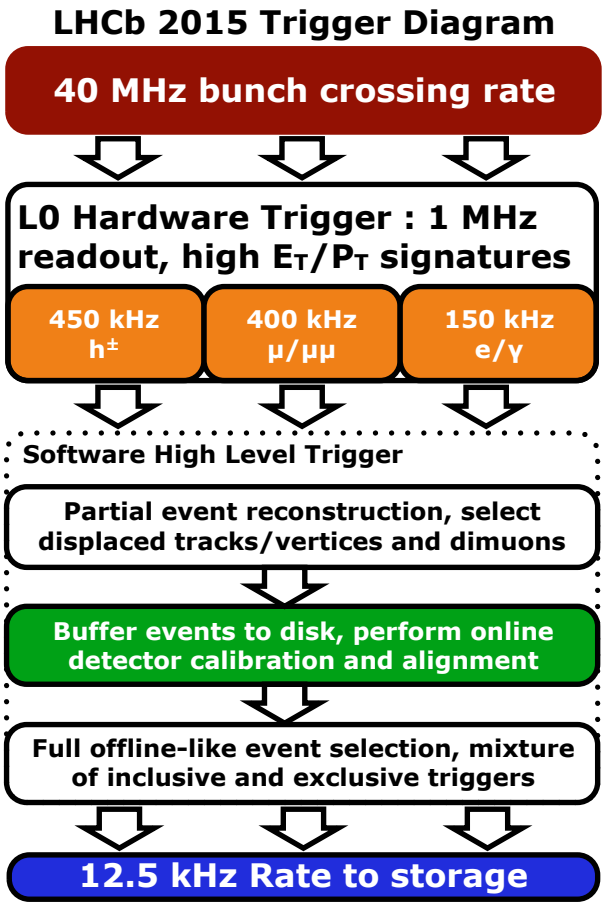

LHCb upgrade trigger (2020)

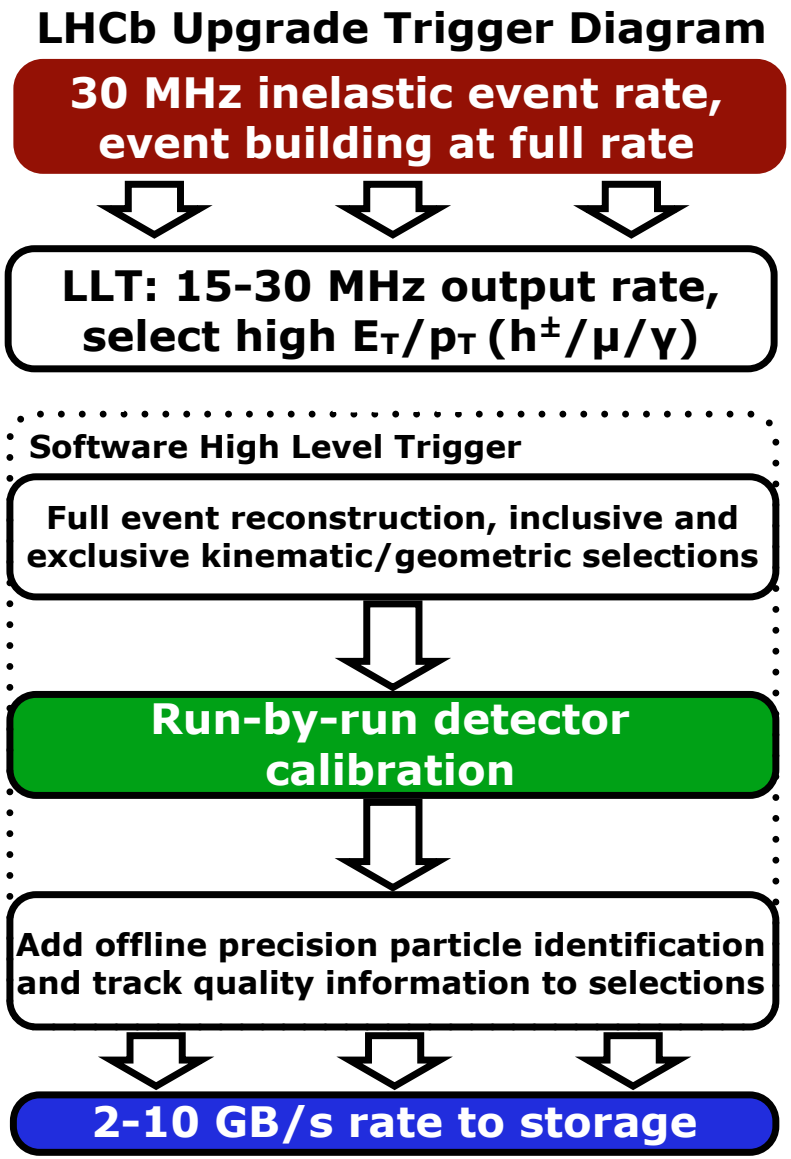

LHCb Vertex detector

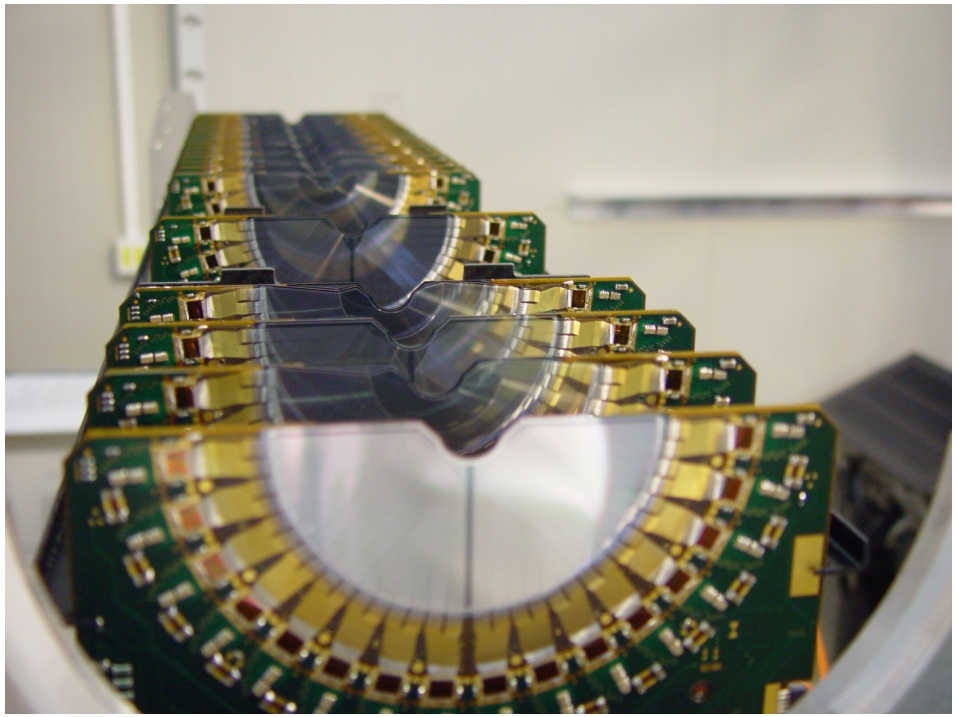

21 (+2) Silicon disks (42 +4 modules).
8.2 mm from the beam axis. 300 μm thick. Strip pitches 37$-$97 μm

Some LHCb expectations on $R(X_c)$

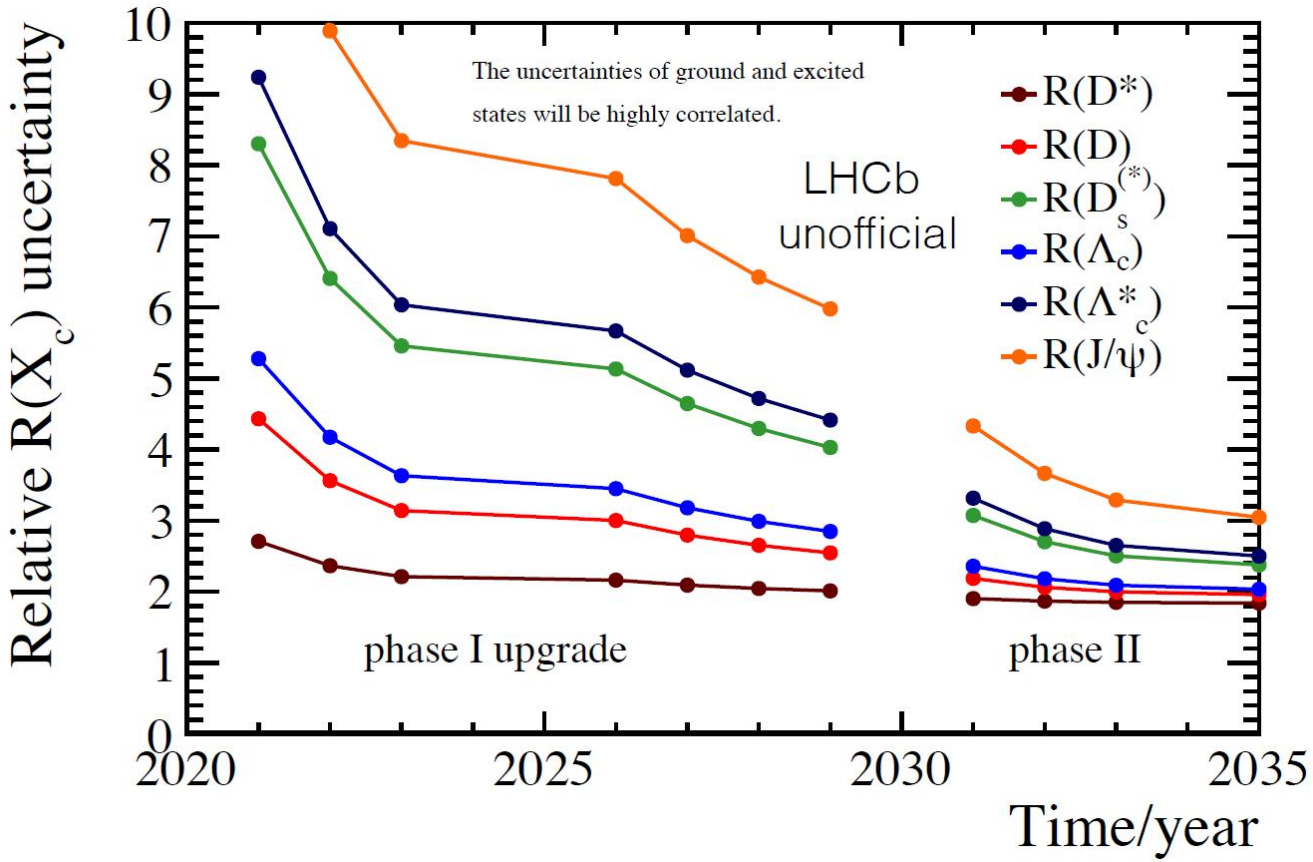

- Above are only crude estimates, to be refined soon.
- Other observables than $R(X_c)$ available to study NP: angles, $BR(q^2)$, polarization, ...
- Samples with high signal purity can be obtained, in particular using hadronic τ decays

BaBar 2012 result

[PRL 109, 101802 (2012)]

Decay	$N_{\rm sig}$	$N_{\rm norm}$	$\varepsilon_{\rm sig}/\varepsilon_{\rm norm}$	$\mathcal{R}(D^{(*)})$	$\mathcal{B}(B \to D^{(*)}\tau\nu)(\%)$	$\Sigma_{\rm stat}$	$\Sigma_{\rm tot}$
$B^- \to D^0\tau^-\bar{\nu}_\tau$	314 ± 60	1995 ± 55	0.367 ± 0.011	$0.429 \pm 0.082 \pm 0.052$	$0.99 \pm 0.19 \pm 0.13$	5.5	4.7
$B^- \to D^{*0}\tau^-\bar{\nu}_\tau$	639 ± 62	8766 ± 104	0.227 ± 0.004	$0.322 \pm 0.032 \pm 0.022$	$1.71 \pm 0.17 \pm 0.13$	11.3	9.4
$\bar{B}^0 \to D^+\tau^-\bar{\nu}_\tau$	177 ± 31	986 ± 35	0.384 ± 0.014	$0.469 \pm 0.084 \pm 0.053$	$1.01 \pm 0.18 \pm 0.12$	6.1	5.2
$\bar{B}^0 \to D^{*+}\tau^-\bar{\nu}_\tau$	245 ± 27	3186 ± 61	0.217 ± 0.005	$0.355 \pm 0.039 \pm 0.021$	$1.74 \pm 0.19 \pm 0.12$	11.6	10.4
$\bar{B} \to D\tau^-\bar{\nu}_\tau$	489 ± 63	2981 ± 65	0.372 ± 0.010	$0.440 \pm 0.058 \pm 0.042$	$1.02 \pm 0.13 \pm 0.11$	8.4	6.8
$\bar{B} \to D^*\tau^-\bar{\nu}_\tau$	888 ± 63	11953 ± 122	0.224 ± 0.004	$0.332 \pm 0.024 \pm 0.018$	$1.76 \pm 0.13 \pm 0.12$	16.4	13.2

$$N(B^0 \to D^{*-}\tau^+\nu_\tau) = 245 \pm 27$$

Belle II Projections

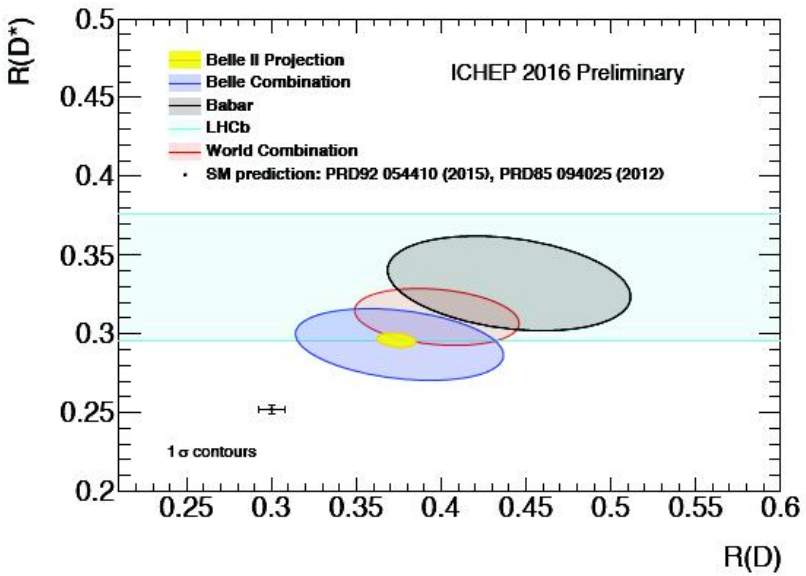

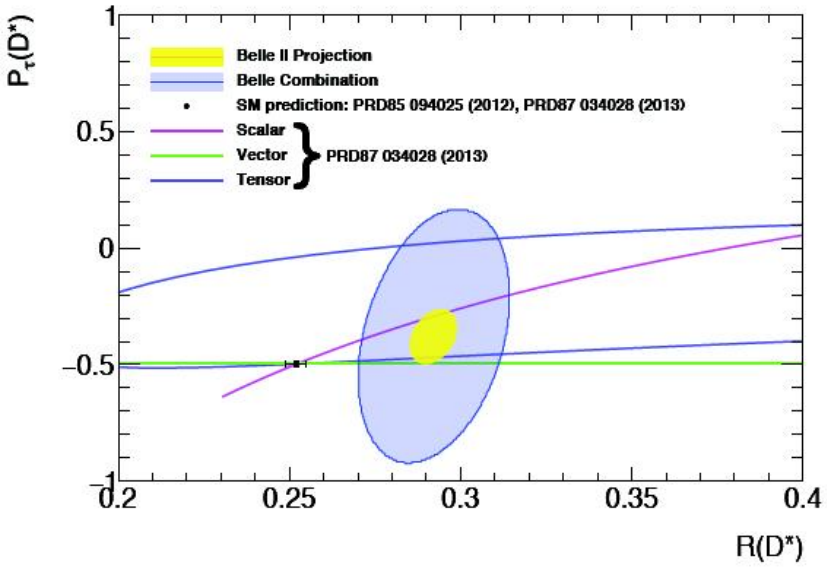

	ΔR(D) [%]			ΔR(D*) [%]		
	Stat	Sys	Total	Stat	Sys	Total
Belle 0.7 ab^{-1}	14	6	16	6	3	7
Belle II 5 ab^{-1}	5	3	6	2	2	3
Belle II 50 ab^{-1}	2	3	3	1	2	2

- SL- & Had- tag full sim sensitivity studies in progress.
- Projections based on Belle + assumed $R(D)_{SL}$ precision
- SL background modelling will dominate error @ 50 ab^{-1}.

LFU prospects using semitauonic decays at LHCb

- More statistics: Run 2 will bring a factor 5 in stat with respect to Run 1.
  Then very large samples expected with Run 3, 4, 5 and until 2037.
  Many systematics will reduce with larger samples. Other will benefit from BESSIII and Belle II measurements.

- More observables: In the future, interest will shift towards new observables beyond the branching fraction ratio: angles, $R(X_c)(q^2)$.
  Angular analysis would allow to determine spin structure of potential NP contribution.

  High purity samples ($> 50\%$) already achievable using hadronic mode.

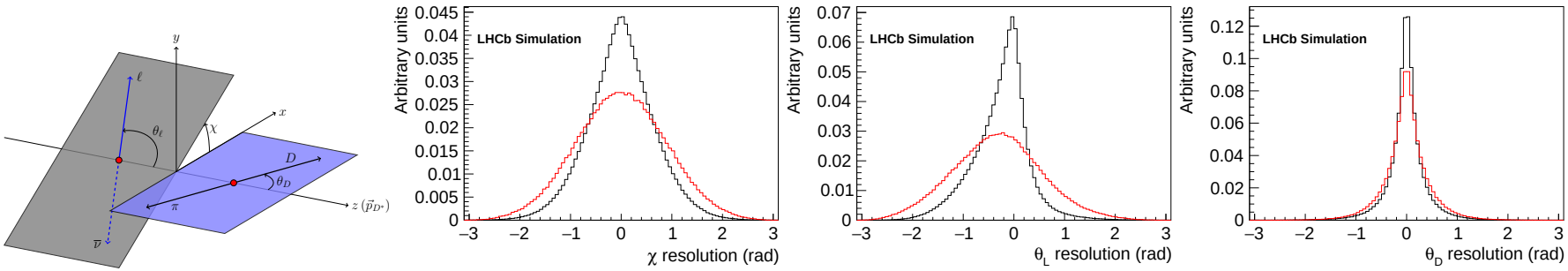

Angular resolution for simulated $B \to D^* \mu\nu$ (black) and $B \to D^* \tau\nu$ (red) decays, with $\tau^+ \to \mu^+ \nu_\mu \nu_\tau$

- More channels:
  - $b \to c\tau\nu$: $R(D^+)$, $R(D^0)$, $R(D_s^{-(*)})$, $R(\Lambda_c^{(*)})$, ...
  - $b \to u\tau\nu$: $R(\Lambda_b^0 \to p\tau\nu)$, $R(B \to pp\tau\nu)$, ...